Interaction of the N terminus of ADP-ribosylation factor with the PH domain of the GTPase-activating protein ASAP1 requires phosphatidylinositol 4,5-bisphosphate

Received for publication, May 8, 2019, and in revised form, October 2, 2019 Published, Papers in Press, October 6, 2019, DOI 10.1074/jbc.RA119.009269

Neeladri Sekhar Roy[‡], Xiaoying Jian[‡], Olivier Soubias[§], Peng Zhai[‡1], Jessica R. Hall[¶2], Jessica N. Dagher[¶3], Nathan P. Coussens[¶], Lisa M. Jenkins[‖], Ruibai Luo[‡], Itoro O. Akpan[‡], Matthew D. Hall[¶], R. Andrew Byrd[§], Marielle E. Yohe[‡4], and Paul A. Randazzo[‡5]**

*From the [‡]Laboratory of Cellular and Molecular Biology, [‖]Laboratory of Cell Biology, and [§]Structural Biophysics Laboratory, Center for Cancer Research, NCI, National Institutes of Health, Frederick, Maryland 21702, the [¶]Chemical Genomics Center, National Center for Advancing Translational Sciences, National Institutes of Health, Bethesda, Maryland 20892, and the **Pediatric Oncology Branch, Center for Cancer Research, NCI, National Institutes of Health, Bethesda, Maryland 20892*

Edited by Alex Toker

Arf GAP with Src homology 3 domain, ankyrin repeat, and pleckstrin homology (PH) domain 1 (ASAP1) is a multidomain GTPase-activating protein (GAP) for ADP-ribosylation factor (ARF)-type GTPases. ASAP1 affects integrin adhesions, the actin cytoskeleton, and invasion and metastasis of cancer cells. ASAP1's cellular function depends on its highly-regulated and robust ARF GAP activity, requiring both the PH and the ARF GAP domains of ASAP1, and is modulated by phosphatidylinositol 4,5-bisphosphate (PIP_2). The mechanistic basis of PIP_2-stimulated GAP activity is incompletely understood. Here, we investigated whether PIP_2 controls binding of the N-terminal extension of ARF1 to ASAP1's PH domain and thereby regulates its GAP activity. Using [Δ17]ARF1, lacking the N terminus, we found that PIP_2 has little effect on ASAP1's activity. A soluble PIP_2 analog, dioctanoyl-PIP_2 ($diC8PIP_2$), stimulated GAP activity on an N terminus–containing variant, [L8K]ARF1, but only marginally affected activity on [Δ17]ARF1. A peptide comprising residues 2–17 of ARF1 ([2–17]ARF1) inhibited GAP activity, and PIP_2-dependently bound to a protein containing the PH domain and a 17-amino acid-long interdomain linker immediately N-terminal to the first β-strand of the PH domain. Point mutations in either the linker or the C-terminal α-helix of the PH domain decreased [2–17]ARF1 binding and GAP activity. Mutations that reduced ARF1 N-terminal binding to the PH domain also reduced the effect of ASAP1 on cellular actin remodeling. Mutations in the ARF N terminus that reduced binding also reduced GAP activity. We conclude that PIP_2 regulates binding of ASAP1's PH domain to the ARF1 N terminus, which may partially regulate GAP activity.

ASAP1 is a GTPase-activating protein (GAP)[6] for ADP-ribosylation factor (Arf) GTPases (1, 2). It is composed of BAR, PH, Arf GAP, ankyrin repeat, proline-rich, E/DLPPKP repeat, and SH3 domains. In cells, ASAP1 controls integrin adhesion complexes and actin remodeling (3–7). ASAP1 has been found to affect cell behaviors dependent on adhesions and actin, including proliferation, invasion, and metastasis of cancer cells (3, 8–13). The cellular function of ASAP1 depends on its highly-regulated and robust Arf GAP activity, which refers to the enzymatic activity of converting Arf·GTP to Arf·GDP. The phosphoinositide PIP_2 increases enzymatic power from $\approx 10^4\ M^{-1}\ s^{-1}$ to greater than $10^8\ M^{-1}\ s^{-1}$ (14, 15). PIP_2-dependent activity of ASAP1 requires the PH domain that is immediately N-terminal to the catalytic Arf GAP domain (16, 17).

Over 300 proteins in humans contain PH domains (18–21), which are composed of a sandwich of seven β-strands capped at one end by an α-helix. Proteins with PH domains regulate signaling, membrane trafficking, and the actin cytoskeleton (22–24). Approximately 15% of PH domains bind to phosphoinositides (25). They can also bind to small GTPases (24), such as Arf (26–31) and other PH domains, as with DOK7 (docking protein 7) to mediate homodimerization (32). They have also been reported to bind to a phosphoinositide and protein simultaneously, functioning as a coincidence detector (27).

PH domains have been found to control protein function by one of three mechanisms. First, proteins can be recruited to surfaces by

This work was supported by NCI Intramural Program Project BC-007365 from the National Institutes of Health (to R. A. B., M. D. H., M. E. Y., and P. A. R.), an Alex's Lemonade Stand Foundation Young Investigators Award, and by the NCI Rasopathies Initiative from the National Institutes of Health (to M. E. Y.). The authors declare that they have no conflicts of interest with the contents of this article.

This article contains Figs. S1–S3.

[1] Present address: Dept. of Human and Molecular Genetics, Virginia Commonwealth University, Richmond, VA 23298.

[2] Present address: Dept. of Biology, Wake Forest University, Winston-Salem, NC 27109.

[3] Present address: Novo Nordisk, Beijing 100020, China.

[4] To whom correspondence may be addressed: Pediatric Oncology Branch, NCI, National Institutes of Health, Bethesda, MD 20892. E-mail: Marielle.Yohe@nih.gov.

[5] To whom correspondence may be addressed. E-mail: randazzp@mail.nih.gov.

[6] The abbreviations used are: GAP, GTPase-activating protein; Arf, ADP-ribosylation factor; Arl, Arf-like GTPase; BAR, Bin/amphiphysin/RVS; CDR, circular dorsal ruffles; DH, Dbl homology; $diC8PIP_2$, dioctanoyl PIP_2; EDANS, 5-[(2-aminoethyl)amino]naphthalene-1-sulfonic acid; EDC, 1-ethyl-3-(3-dimethylaminopropyl) carbodiimide hydrochloride; HVR, hypervariable region; HMQC, heteronuclear multiple quantum correlation; LUV, large unilamellar vesicle; MSP, membrane scaffolding protein; PA, phosphatidic acid; PDB, Protein Data Bank; PDGF, platelet-derived growth factor; PH, pleckstrin homology; PIP_2, phosphatidylinositol 4,5-bisphosphate; PS, phosphatidylserine; PTB, phosphotyrosine binding; TAMRA, carboxylic acid of tetramethylrhodamine; ND, nanodisc.

their PH domains binding to membrane components, including phosphoinositides and GTPases (20, 24, 26, 27, 30, 33–35). Recruitment concentrates and orients the protein on a surface that contains a target molecule. In addition, PH domains can autoinhibit or position other structural elements of a protein to inhibit intramolecular catalytic domains, as described for kinases and guanine nucleotide exchange factors (36–41). For p63RhoGEF, $G\alpha_q$ binding to a C-terminal extension of the PH domain relieves autoinhibition (36). In the case of the Arf exchange factors, cytohesins, cooperative binding of phosphoinositide and Arf6·GTP or Arl4·GTP to the PH domain relieves PH domain–mediated autoinhibition (29, 39, 42). Finally, as is observed in some exchange factors, PH domains or extensions of the PH domain can contribute directly to binding the substrate protein (43, 44).

The PH domain of ASAP1 might contribute to GAP activity by the third mechanism, through a direct interaction with the substrate. We have found recruitment of the Arf GAP domain to a hydrophobic surface containing the substrate Arf1·GTP is not sufficient for GAP activity, and the cognate PH domain is necessary (16). We have also found that GAP activity requires a unique structural feature of Arf family GTPase, the N-terminal extension from the GTP-binding domain, which has previously been found to bind to ASAP1 (although the binding site has not been determined) (45). Furthermore, the interaction might be regulated by PIP_2. PIP_2 binding to the PH domain is necessary for activity (14, 15, 17, 46). These observations, together with the precedent of cytohesin, in which a phosphoinositide, phosphatidylinositol 3,4,5-trisphosphate, regulates binding of Arf6·GTP to the PH domain (29), have led us to hypothesize that, rather than mediating recruitment to a lipid bilayer, PIP_2 binding to the PH domain of ASAP1 regulates binding to the N terminus of Arf1 to control GAP activity.

Results

Cognate PH domain of ASAP1 and the N terminus of Arf are necessary for PIP_2-stimulated GAP activity

Previously, we found that PIP_2-stimulated activity of a recombinant protein composed of the PH, Arf GAP, and ankyrin repeat domains of ASAP1, [325–724]ASAP1, referred to as PZA (for PH, Zinc binding, which comprises the Arf GAP catalytic domain, and Ankyrin repeat domains, see Fig. 1*A*) by more than 10,000-fold (14). In addition, we found that (i) the cognate PH domain of ASAP1 is required for activity (16); (ii) membrane recruitment is not sufficient for activity (16, 17); and (iii) Arf1 lacking its N-terminal 17 amino acids is a poor substrate (see Fig. 1*A* for sequence of the N terminus) (45). The N terminus of native Arf1 is myristoylated. To explore the role of the N terminus of Arf1 for PIP_2-stimulated GAP activity of ASAP1, PZA was titrated into reaction mixtures containing myrArf1·GTP, nonmyrArf1, or [Δ17]Arf1·GTP and large unilamellar vesicles (LUVs) with or without incorporated phosphatidylserine (PS), which reduces the concentration of PIP_2 needed for maximum activation (14). GAP activity is reported as the C_{50}, which is the concentration of PZA needed to induce 50% of the GTP bound to Arf1 to be hydrolyzed in 3 min and is inversely related to enzymatic power (Fig. 1*B* and Table 1) (47, 48). For myrArf1, as we have previously found, there was a greater than 10,000-fold difference between the C_{50} values measured in the absence and presence of PIP_2. Results using nonmyristoylated Arf1 were similar. In contrast, the difference was 2-fold for [Δ17]Arf1. We then determined if the results extrapolated to full-length ASAP1. We were not able to achieve as high a concentration of the full-length protein as we were with PZA, which limited the titrations. Nevertheless, the data were sufficient to conclude that the PIP_2 dependence of full-length ASAP1 and PZA was similar and that [Δ17]Arf was a poor substrate for full-length ASAP1 (Fig. 1*B*). Given the importance of an intact N terminus of Arf1 for PIP_2-stimulated activity, we considered that a peptide derived from the N terminus of Arf1 ([2–17]Arf1) might affect activity. We found that [2–17]Arf1 inhibited activity with an IC_{50} of 5.6 ± 0.6 μM (Fig. 1*C*). A peptide composed of the same amino acids but in a scrambled order ([2–17]scrambled) was more than 15-fold less efficient as an inhibitor. A peptide in which three lysines were replaced with aspartates ([K10D,K15D,K16D, 2–17]Arf1) was also an inefficient inhibitor of GAP activity. Full-length ASAP1 was similarly inhibited by [2–17]Arf1 but not [2–17]scrambled (Fig. 1*C*). Thus, PIP_2-stimulated GAP activity required that Arf1 have an intact N terminus and was specifically inhibited by a peptide composed of the isolated Arf1 N terminus.

PIP_2-dependent activity is independent of a lipid surface

The myristoylated N terminus of Arf1 mediates recruitment to surfaces (49–51) and binds to PIP_2 (52, 53). Therefore, part of the difference in GAP activity against full-length myristoylated Arf1 and [Δ17]Arf1 might be due to lack of recruitment of [Δ17]Arf1 to the surface containing ASAP1. To determine whether there was a recruitment-independent component of PIP_2 activation, we sought conditions that would allow us to measure activity without LUVs. When bound to GTP, full-length Arf1 is not stable without a hydrophobic surface, but we have previously identified a point mutant of Arf1, [L8K]Arf1, that is stable without a hydrophobic surface (45). [L8K]Arf1 is as efficient a substrate as WT Arf1 for ASAP1 when the PIP_2 in the reaction is presented in mixed micelles of Triton X-100 (45, 54). [L8K]Arf1 is ~10-fold less efficient as a substrate than WT Arf1 when the PIP_2 in the reaction is incorporated into LUVs. However, GAP activity on [L8K] Arf1, like that on WT Arf1, depends on PIP_2 (Fig. 2*A* and Table 1). Importantly, the GAP activity of ASAP1 with [L8K]Arf1 as a substrate is inhibited by the [2–17]Arf1 peptide, with an IC_{50} of 0.8 ± 0.1 μM, but not by the [2–17]scrambled peptide (Fig. 2*B*). A second consideration for examining activity without a hydrophobic surface is the soluble PIP_2 analog. In crystal structures of the ligand-bound and unliganded forms of the PH domain (14), PIP_2 binds to two sites, the canonical site and the atypical site. These two binding sites are separated from one another by the loop between β-strands 1 and 2, the structure of which is stabilized by isoleucine 353. We considered that there may be a minimal length of the acyl group of PIP_2 required to stabilize the loop and support GAP activity. We tested [L8K]Arf1 as a substrate with either no PIP_2 or 200 μM diC4PIP_2, diC6PIP_2, or diC8PIP_2, which all have critical micelle concentrations greater than 1 mM (55, 56).[7] We

[7] We determined the critical micelle concentration for diC8PIP_2 to be >1 mM, using the method described in Ref. 57.

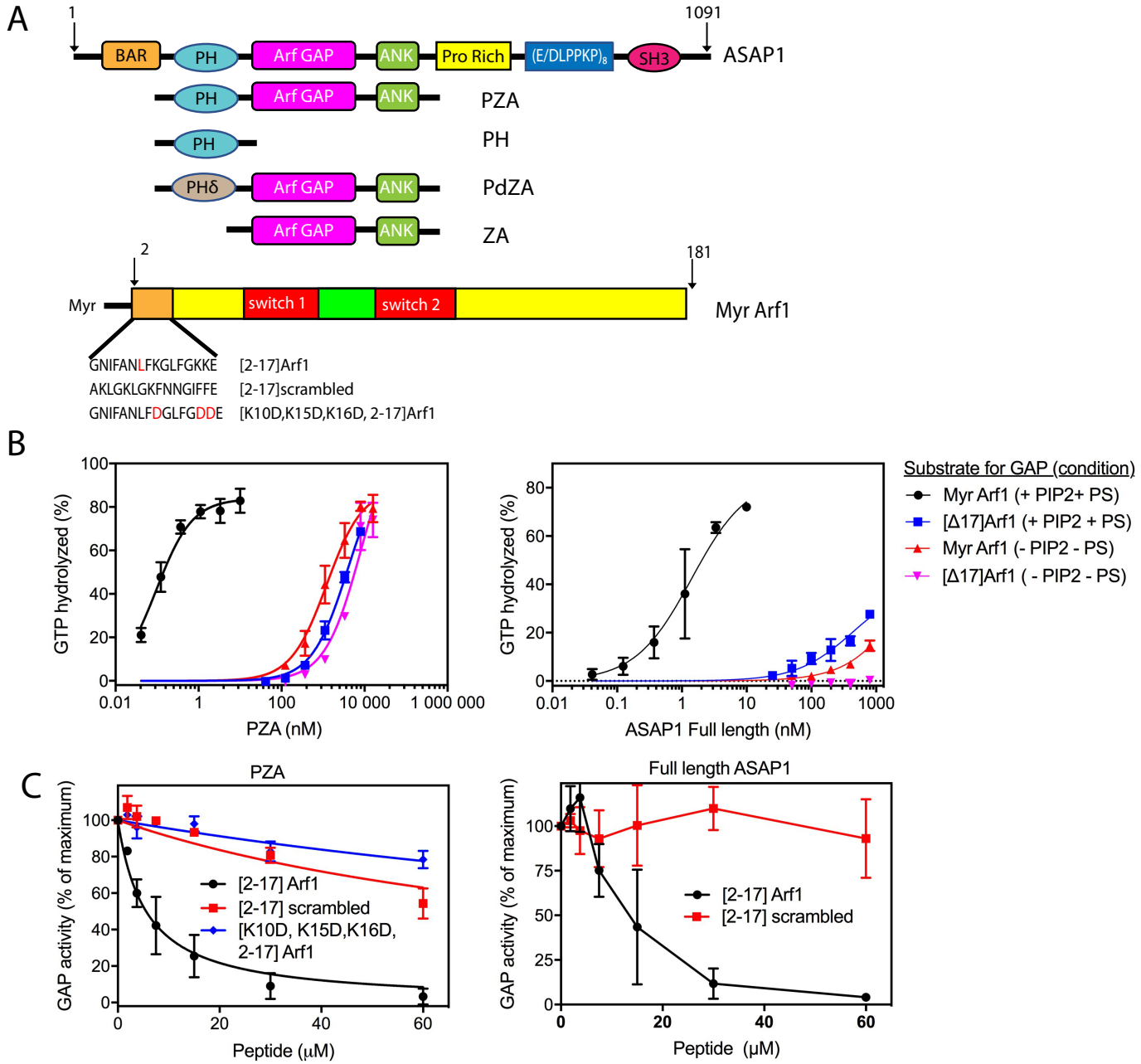

Figure 1. N-terminal extension of Arf1 is necessary for PIP$_2$-stimulated ASAP1 GAP activity. *A*, schematic of recombinant proteins used in this paper. The domain structure of ASAP1 is shown in the *schematic at top*. Abbreviations used are: *BAR*, Bin/amphiphysin/RVS; *PH*, pleckstrin homology; *Arf GAP*, Arf GTPase-activating protein; *ANK*, ankyrin repeat; *Pro-Rich*, proline-rich; (*E/DLPPKP*)$_8$, tandem repeats of E/DLPPKP; *SH3*, Src homology 3. Recombinant proteins used in the studies are shown *below the schematic* of full-length ASAP1. *PH*$_\delta$ is for the PH domain of phospholipase Cδ1. The acronyms for the proteins include "Z" for the Arf GAP domain, which is a zinc-binding motif, and "Pd" for the PH domain of phospholipase Cδ1. *Below* the ASAP1-derived proteins, a representation of Arf1 and the amino acids comprising the N-terminal 2–17 residues, the same amino acids in a scrambled sequence, and the sequence with lysines changed to aspartates are shown. *B*, comparison of PIP$_2$-stimulated GAP activity of ASAP1 using full-length Arf1 and [Δ17]Arf1 as substrates. PZA (*left panel*) or full-length ASAP1 (*right panel*) was titrated into a GAP reaction containing 0.1 μM full-length Arf1 or [Δ17]Arf1 and LUVs at a total phospholipid concentration of 500 μM containing 15% PS, 5% PIP$_2$, or without PS or PIP$_2$, as indicated. The summary of three experiments is shown for PZA and two experiments for full-length ASAP1. *Error bars* are S.E. *C*, inhibition of Arf GAP activity by an N-terminal peptide of Arf1. A peptide comprising amino acids 2–17 of Arf1 ([2–17]Arf1), a peptide of the same amino acid composition but with a scrambled sequence ([2–17]scrambled), or [2–17]Arf 1 with the indicated amino acid changes (see *A* for sequences) were titrated into a mixture containing 0.1 μM myrArf1, LUVs at a total phospholipid concentration of 500 μM containing 15% PS, 5% PIP$_2$, and either PZA (0.3 nM) (*left panel*) or full-length ASAP1 (1.4 nM) (*right panel*) sufficient to induce ~50% of the GTP bound to Arf to be hydrolyzed in a fixed time used for the assay in the absence of peptide. Activity in the absence of peptide for PZA was 0.4 and 0.44 min^{-1} for full-length ASAP1. The activity in the absence of peptide was taken to be maximum GAP activity (100%). The summary of three experiments is shown for PZA and two for full-length ASAP1. *Error bars* are S.E.

observed that PIP$_2$ analogs increased activity dependent on acyl length, with more than a 7,000-fold increase in activity with diC8PIP$_2$ compared with no PIP$_2$ (Fig. 2*C* and Table 2). Titration of diC8PIP$_2$ revealed a sigmoidal dependence for PIP$_2$-stimulated activity with a Hill coefficient of 1.9 ± 0.27 (S.E.) (Fig. 2*D*), consistent with previous studies identifying two PIP$_2$-

Table 1

PIP_2-stimulated GAP activity using full-length myristoylated Arf1, full-length nonmyristoylated Arf1, and [Δ17]Arf1 as substrates and [L8K]Arf1

PZA ((325–724)ASAP1) was titrated into a GAP reaction using 0.1 μM full-length myrArf1·GTP, nonmyrArf1·GTP, [L8K]Arf1·GTP, or [Δ17]Arf1·GTP as substrates and LUVs at a total phospholipid concentration of 500 μM without PS or PIP_2 or with 2.5% PIP_2 and 15% PS, as indicated. The percent of GTP hydrolyzed was plotted against PZA concentration and fit to a hyperbola using GraphPad Prism 7.0 to estimate C_{50} values. The values are the average of three experiments ± S.E. The raw data are shown in Fig. S1.

	$C_{50\ (nM)}$	
Substrate	LUV (−PIP2 −PS)	LUV (+PIP2 +PS)
myrArf1	1200 ± 170	0.10 ± 0.01
nonmyrArf	880 ± 170	0.27 ± 0.07
[Δ17]Arf1	8100 ± 2400	4000 ± 400
[L8K]Arf1	5100 ± 1500	1.5 ± 0.3

binding sites on the ASAP1 PH domain (14) and at least one on Arf1 (52, 53, 58) that are necessary to form the active complex.[8] There were some differences in the specificity of headgroups for stimulating GAP activity between the water-soluble phospholipid analogs and LUVs. For instance, diC8-phosphatidylserine (PS) increased activity by 1000-fold (Table 2), compared with 15-fold for PS in LUVs (14).[9] Nevertheless, the N terminus of Arf1 was critical for the observed activation as it was in LUVs. diC8PIP_2 stimulated the activity of [L8K]Arf1, which has the N-terminal extension from the GTP-binding domain, more than 7,000-fold, but only 3-fold for [Δ17]Arf1, which does not have the extension (Fig. 2*E* and Table 3). The cognate PH domain was required as protein composed of the Arf GAP and ankyrin repeat domains (ZA) or the PH domain of PLCδ1 and the Arf GAP and ankyrin repeats of ASAP1 (PdZA, see Fig. 1*A* for a schematic of the proteins) had little or no activity in the presence of LUVs or diC8PIP_2 (Fig. 2, *F* and *G*). As for activity measured with PIP_2 in LUVs, [2–17]Arf1, but not [2–17]scrambled, inhibited diC8PIP_2-stimulated activity with an IC_{50} of 4.7 ± 0.4 μM (Fig. 2*H*). Although there are differences between the reaction with diC8PIP_2 and LUVs, which we are pursuing in other studies,[9] our results indicate that the N termini of Arf1 and PH domain are critical for catalysis whether PIP_2 is presented in LUVs or as the soluble analog diC8PIP_2.

PIP_2 controls direct binding of the N terminus of Arf to the PH domain of ASAP1

The N terminus of Arf1 and the PH domain of ASAP1 are critical for PIP_2-stimulated activity by a mechanism that may not only depend on recruitment to a surface. We hypothesized that GAP activity is controlled by PIP_2-dependent binding of the N terminus of Arf1 to the PH domain of ASAP1 (schematic of the hypothesis is shown in Fig. 3). As a test of the hypothesis, we used three complementary assays (Figs. 4–6) to determine whether there is direct association between the ASAP1 PH domain and [2–17]Arf1. First, we measured interaction by Förster resonance energy transfer (FRET, see Fig. 4*A* for schematic of assay). The fluorophore 5-[(2-aminoethyl)-amino]naphthalene-1-sulfonic acid (EDANS, peak excitation wavelength 336 nm, emission peak 490 nm) was covalently linked to the C terminus of [2–17]Arf1. EDANS is an acceptor for FRET from tryptophan, which absorbs light at 280 nm and emits at a peak of ~340 nm. PH_{ASAP1} contains two tryptophans (Trp-357 and Trp-422, see Fig. 4*B* for structure of PH domain). Given the dimensions of the PH domain, either tryptophan could act as a donor for EDANS if the modified peptide bound to the surface of the PH domain. PH_{ASAP1} was incubated with 200 μM diC8PIP_2 and the indicated concentrations of [2–17]Arf1-EDANS. The solution was excited with 280 nm light, and an emission spectrum was measured. Representative spectra are shown in Fig. 4*C*, and a summary of three experiments with calculated FRET efficiencies is shown in Fig. 4*D*. In the absence of [2–17]Arf1-EDANS, a single peak is observed with a maximum of ~340 nm (Fig. 4*C*), as expected for fluorescence emission from tryptophan. Addition of [2–17]Arf1-EDANS induced a concentration-dependent decrease in emission at 340 nm and a concomitant increase in emission at 490 nm, indicating FRET. Titrating peptide, we used quenching of tryptophan fluorescence to quantify FRET. We found the FRET signal was saturable with a half-maximum effect at 2.3 ± 0.14 μM [2–17]Arf1-EDANS (Fig. 4*D*), similar to the concentration dependence observed for inhibition of GAP activity. Similar results were obtained with EDANS linked to the N terminus of [2–17]Arf1 (not shown). No FRET signal was observed with [2–17]scrambled EDANS (Fig. 4*D*). One would predict that [2–17]Arf1 without EDANS would compete with [2–17]Arf1-EDANS for binding to PH_{ASAP1}, reducing FRET. [2–17]Arf1 or [2–17]scrambled without fluorophore were titrated into a reaction containing 1 μM PH_{ASAP1}, 4 μM [2–17]Arf1-EDANS, and 200 μM diC8PIP_2 (Fig. 4*E*). We found [2–17]Arf1, but not [2–17]scrambled, competed with [2–17]Arf1-EDANS to reduce FRET. Like the stimulation in GAP activity, binding, as determined by FRET, depended on diC8PIP_2 (Fig. 4*F*) with a Hill coefficient of 1.4 ± 0.15. [R360Q]PZA, a mutant with reduced affinity for PIP_2, had a lower affinity for [2–17]Arf1-EDANS than PZA (Fig. 4*G*). For experiments with full-length ASAP1, quenching of tryptophan fluorescence was not a sensitive measure of FRET because there are six tryptophans in ASAP1 outside of the PH domain, the putative binding site for the peptide. Therefore, we titrated ASAP1 into the reaction and measured FRET as an increase in emission from the acceptor, EDANS, at 493 nm. FRET was observed when titrating full-length ASAP1 into a solution containing [2–17]Arf1-EDANS but not with [2–17]scrambled-EDANS (Fig. 4*H*). FRET was not observed between $PH_{PLC\delta1}$ and [2–17]Arf1-EDANS (Fig. 4*D*). Taken together, these data are interpreted as a specific PIP_2-dependent association between PH_{ASAP1} and [2–17]Arf1.

Fluorescence anisotropy (59) was used as a complementary assay to detect binding between [2–17]Arf1 and PH_{ASAP1}. The principle of the assay is shown in Fig. 5*A*. A molecule with a fluorophore is incubated with a binding partner. The sample is excited with plane polarized light, and emission is measured along axes parallel and perpendicular to the plane of excitation. If the fluorophore does not tumble between the time of excitation and emission, emission is polarized with a consequent difference in emission intensity between the perpendicular planes,

[8] We also observed binding of diC8PIP_2 to [2–17]Arf1 by circular dichroism spectrometry (not shown).

[9] The differences between GAP activity in LUVs and with PIP_2 analogs are described in more detail in a manuscript currently in preparation (N. S. Roy, X. Jian, R. Luo, P. A. Randazzo, and M. E. Yohe).

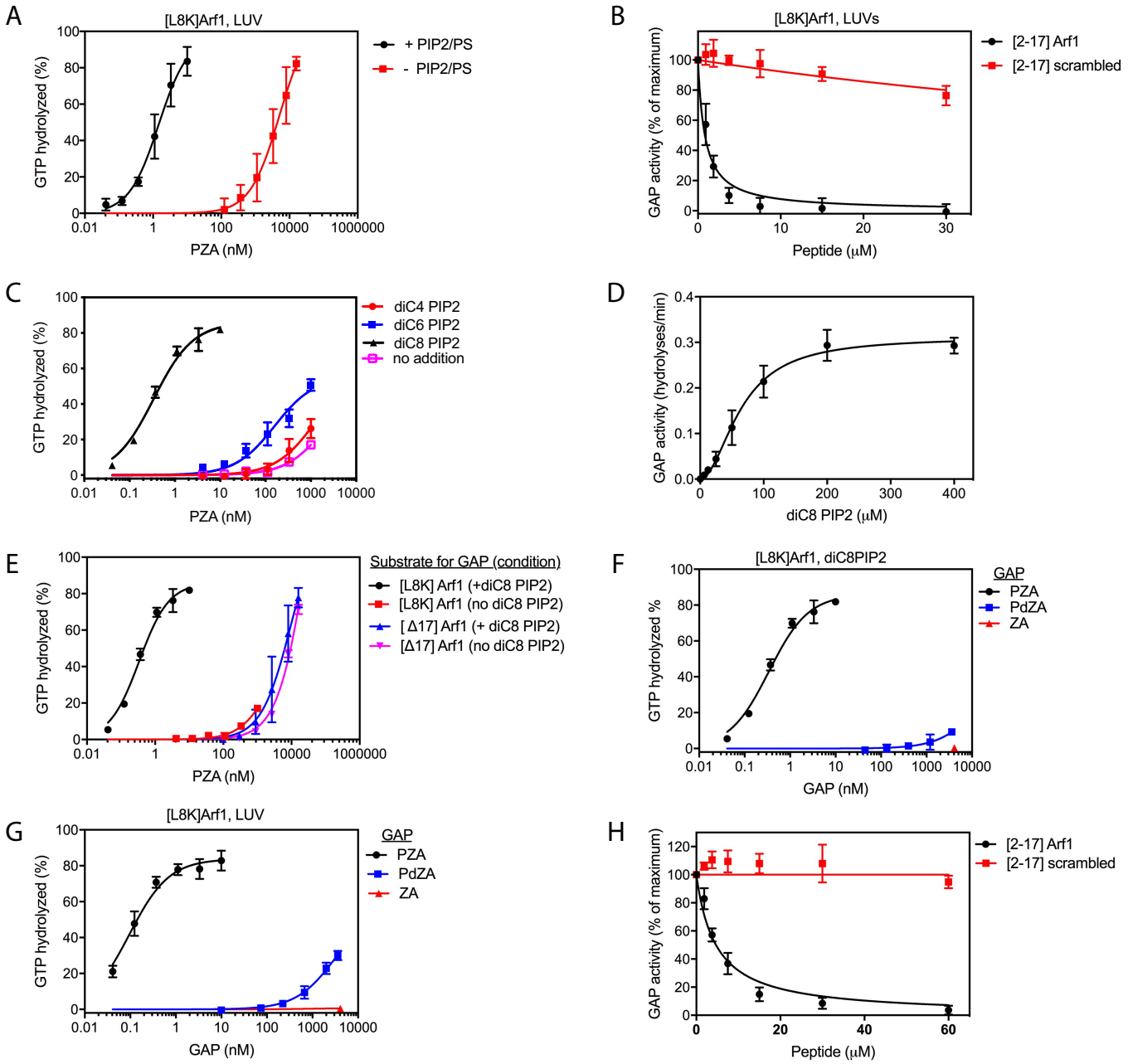

Figure 2. PIP$_2$-stimulated activity does not depend on a hydrophobic surface. *A,* [L8K]Arf1 is a substrate for PIP$_2$-dependent ASAP1 GAP activity. PZA was titrated into a reaction containing [L8K]Arf1·GTP and LUVs with and without PS and PIP$_2$ as described in Fig. 1*B*. *B,* [2–17]Arf1 inhibits ASAP1 GAP activity against [L8K]Arf1. The effect of [2–17]Arf1 and [2–17]scrambled on GAP activity was determined as described in Fig. 1*C*. The concentration of PZA in the reactions was 3 nM, and the activity in the absence of peptide was 0.32 min^{-1}. *C,* dependence of Arf GAP activity on acyl chain length of PIP$_2$ analogs. PZA was titrated into a reaction containing 0.1 μM [L8K]Arf1·GTP and 200 μM PIP$_2$ analogs with the indicated acyl groups. GTP hydrolysis in 3 min was determined. *D,* diC8PIP$_2$ dependence of GAP activity. diC8PIP$_2$ was titrated into a reaction containing 0.5 nM PZA and 0.1 μM [L8K]Arf1. GTP hydrolysis in 3 min was determined. *E,* comparison of diC8PIP$_2$-stimulated GAP activity using [L8K]Arf1 and [Δ17]Arf as substrates. PZA was titrated into a reaction containing either 0.1 μM [L8K]Arf1·GTP or [Δ17]Arf1·GTP and either no PIP$_2$ or 200 μM diC8PIP$_2$. *F* and *G,* cognate PH domain of ASAP1 is required for activity with PIP$_2$ in LUVs and diC8PIP$_2$. PZA, ZA, or PdZA were titrated into a mixture containing either diC8PIP$_2$ and 0.1 μM [L8K]Arf1·GTP (*F*) or LUVs with PS and PIP$_2$ and 0.1 μM myrArf1·GTP (*G*). *H,* inhibition of diC8PIP$_2$-stimulated GAP activity by [2–17]Arf1. The experiment was performed as described in Fig. 1*C* with [2–17]Arf1 or [2–17]scrambled using diC8PIP$_2$ to stimulate activity and 0.1 μM [L8K]Arf1·GTP as substrate. The concentration of PZA was 0.5 nM. Activity with no peptide was 0.32 min^{-1}. Results shown are the summary of three experiments. *Error bars* are S.E.

or anisotropy. Random tumbling of the fluorophore between the time of excitation and emission reduces anisotropy, while binding of a small fluorophore-containing molecule to a larger molecule would slow rotation, increasing anisotropy. [2–17]Arf1 covalently linked through a lysine added to the C terminus to the fluorophore, tetramethylrhodamine(TAMRA), was incubated with PZA, ZA, PH$_{ASAP1}$, or PdZA and 200 μM diC8PIP$_2$. The samples were excited with polarized light, and anisotropy was measured (Fig. 5*B*). When PH$_{ASAP1}$ or PZA were titrated into the solution, a saturable increase in anisotropy was observed with a half-maximal effect at 6.5 ± 2.6 and 3.2 ± 0.9 μM, respectively, consistent with the K_d value measured by FRET. ZA and PdZA had no detectable effect on anisotropy of [2–17]Arf1-TAMRA.

Table 2

Dependence of GAP activity on acyl chain length and headgroup of phospholipid analogs

PZA was titrated into a reaction using 0.1 μM [L8K]Arf1·GTP as substrate and 200 μM of the indicated lipid analog. GTP hydrolysis in 3 min was determined. The percent of GTP hydrolyzed was plotted against PZA concentration and fit to a hyperbola to estimate C_{50} values. The values are the average of three experiments. The raw data are shown in Fig. S2.

Lipid analog	C_{50}
	*n*M
No addition	2200 ± 1208
diC4PIP$_2$	1200 ± 730
diC6PIP$_2$	160 ± 35
diC8PIP$_2$	0.3 ± 0.03
diC8PS	2.1 ± 0.51
diC8PA	6.6 ± 2.8

Table 3

diC8 PIP$_2$-stimulated GAP activity using [L8K]Arf1 and [Δ17]Arf as substrates

PZA was titrated into a GAP reaction using either 0.1 μM [L8K]Arf1·GTP or [Δ17]Arf1·GTP as substrate and 200 μM diC8 PIP$_2$ where indicated. GTP hydrolysis in 3 min was determined. The percent of GTP on Arf that was hydrolyzed was plotted against PZA concentration and fit to a hyperbola to estimate C_{50} values. The data for [L8K]Arf1 are from Table 2. The values are the average of three experiments. The raw data are shown in Fig. S3.

Substrate	$C_{50\ (nM)}$	
	−PIP$_2$	+diC8PIP$_2$
[L8K]Arf1	2200 ± 1200	0.3 ± 0.03
[Δ17]Arf1	29000 ± 6100	9500 ± 3400

To corroborate the FRET and anisotropy results and to establish a suitable assay for high-throughput screening, binding was evaluated by an AlphaScreen® proximity assay (PerkinElmer Life Sciences) (Fig. 6*A*). With this approach, biotinylated [2–17]Arf1 binds streptavidin-conjugated donor beads, whereas polyhistidine-tagged PH$_{ASAP1}$ binds nickel chelate acceptor beads. Upon excitation with 680 nm light, the donor beads generate singlet oxygen. If [2–17]Arf1-biotin binds PH$_{ASAP1}$, the acceptor bead is proximal to the donor bead and able to receive the singlet oxygen, resulting in a chemiluminescent signal at 615 nm (60). The reactions were performed in the presence of diC8PIP$_2$ to facilitate binding between [2–17]Arf1 and PH$_{ASAP1}$. The resulting signal was proportional to the concentration of PH$_{ASAP1}$ in solution (Fig. 6*B*). Titrating nonbiotinylated [2–17]Arf1 to compete with [2–17]Arf1-biotin for binding to the PH domain reduced the signal with a IC_{50} of 5.4 μM [2–17]Arf1 (Fig. 6*C*), consistent with the K_d value measured by FRET and anisotropy.[10]

PIP$_2$-dependent binding of N terminus of Arf1 to the PH domain of ASAP1 correlates with PIP$_2$-dependent GAP activity

As an initial effort to identify the binding determinants between PH$_{ASAP1}$ and [2–17]Arf1, [2–17]Arf1-TAMRA was incubated with the PH domain of ASAP1 ([325–451]ASAP1), diC8PIP$_2$, and the cross-linker EDC. A cross-linked product was identified by SDS-PAGE (data not shown). MS analysis of the product revealed cross-linking between Glu-337 of ASAP1 and Lys-10 of Arf1. The crystal structure revealed that the ASAP1 PH domain has a 17-amino acid N-terminal extension, containing Glu-337, prior to the first β-strand in the canonical fold (Fig. 4*B*) (14). These residues are part of the linker between the BAR and PH domains. Interdomain linkers and extensions of the PH domain contribute to PH domain binding to proteins, for example in cytohesins (29) and p63RhoGAP (36), respectively. We tested the hypothesis that the N-terminal extension of the PH domain of ASAP1 functions to facilitate binding to Arf1 by investigating the binding of the PH domain, including the 17 residues, without 9 of the 17 residues or without 14 of the 17 residues N-terminal to the first β-strand ([325–451]ASAP1, [334–451]ASAP1, and [339–451]ASAP1, respectively) to PIP$_2$ and to [2–17]Arf1. The GAP activities of [325–724]ASAP1, [334–724]ASAP1, and [339–724]ASAP1 were also compared (Fig. 7, *A–D*). The dissociation constants (K_d) of [334–451]ASAP1 and [339–451]ASAP1 for PIP$_2$, measured by binding to sucrose-loaded LUVs with varying concentrations of PIP$_2$, differed by less than a factor of 2 from [325–451]ASAP1. The K_d values of [334–451]ASAP1 and [339–451]ASAP1 for [2–17]Arf1 were 1.7- and 2.5-fold greater than the K_d value of [325–451]ASAP1, determined by FRET. [334–724]ASAP1 and [339–724]ASAP1 had ~1/6th and 1/20th the enzymatic power of [325–724]ASAP1 measured using diC8PIP$_2$, respectively. In LUVs, the difference in activity was 30- and 100-fold. The 100-fold difference in GAP activity between [325–724]ASAP1 and [339–724]ASAP1 was also observed when using nanodiscs as membrane mimetics to present PIP$_2$ (Fig. 7, *E* and *F*) (61). For these experiments, nanodiscs containing PIP$_2$ were titrated into a solution containing ^{13}C-methyl–labeled [325–451]ASAP1 or [339–451]ASAP1, and ^{1}H-^{13}C heteronuclear multiple quantum coherence (HMQC) NMR spectra were collected. Binding of protein to the nanodiscs was detected as a perturbation in the chemical shift of the peak for isoleucine 371. Less than a 2-fold difference between [325–451]ASAP1 and [339–451]ASAP1 was detected (Fig. 7*E*). However, there was a 100-fold difference in activity between the proteins, measured with a GAP assay based on the difference in tryptophan fluorescence between Arf1·GTP and Arf1·GDP (Fig. 7*F*) (61). Based on these results, the linker might contribute to binding, but it is not the major determinant. These results are additional support for the idea that simple recruitment of the Arf GAP domain to a surface containing Arf1·GTP is not sufficient for efficient activation of GAP activity, as there was less than a 2-fold difference for [325–451]ASAP1 and [339–451]ASAP1 in PIP$_2$ binding but a 100-fold difference in PIP$_2$-stimulated GAP activity between [325–724]ASAP1 and [339–724]ASAP1.

We also examined point mutants in an effort to test the prediction that mutations in the PH domain can disrupt [2–17]Arf1 binding and GAP activity without disrupting PIP$_2$ binding (Figs. 4*B* and 8, *A–F*). We selected residues in the N-terminal extension of the PH domain. Two changes were introduced into the linker: (i) glutamine 331, leucine 332, and glutamine 333 were changed to alanines (Q331A,L332A,Q333A), and (ii) glycine 339 was changed to isoleucine (G339I). In addition, we introduced mutations to change aliphatic residues within the α-helix of the PH domain (tyrosine 419 to either alanine or glutamate (Y419A or Y419E), and isoleucine 423 to alanine (I423A). The residues are surface-exposed and near the N-terminal extension of the PH domain that may contribute to binding the N terminus of Arf1. The

[10] High throughput screens for inhibitors using this assay are ongoing.

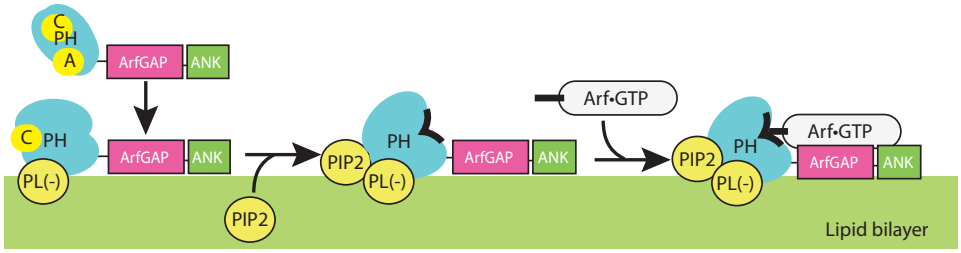

Figure 3. Hypothesized mechanism for PIP$_2$ regulation of GAP activity. In our hypothesis, PIP$_2$ binds to two sites on the PH domain, a canonical site (*C*) and alternate site (*A*) inducing a conformational change in the PH domain that facilitates binding to the N-terminal extension of Arf1. Binding of the N terminus of Arf to the PH domain provides both binding energy and orientation of the GTP-binding domain of Arf in the catalytic pocket.

Y419A mutation did not affect [2–17]Arf1 binding, PIP$_2$ binding, or GAP activity. The other mutations had less than 2-fold effects on PIP$_2$ binding. Effects on [2–17]Arf1 binding correlated with changes in GAP activity. The I423A mutation affected both [2–17]Arf1 binding and GAP activity by 4-fold, the Y419E mutation affected binding by 4.5-fold, and activity by 3-fold and the G339I mutation affected binding by 3-fold and activity by 15-fold. The results are consistent with the hypothesis that GAP activity depends on binding of the N terminus of Arf1 to the PH domain.

Another prediction of the hypothesis is that the introduction of mutations into the N terminus of Arf1 that reduced binding of the N terminus to the PH domain would render Arf1 a less efficient substrate. In contrast to [2–17]Arf1-TAMRA, [K10D,K15D,K16D,2–17]Arf1-TAMRA did not bind to the PH domain, detected as a change in anisotropy (Fig. 8*G*). [L8K,K10D,K15D,K16D]Arf1 was ~1000-fold less efficient a substrate than [L8K]Arf1 (Fig. 8*H*). The correlation of reduced binding with reduced GAP activity is consistent with our hypothesis, although we cannot exclude that the lack of activity was because the mutant Arf1 did not bind PIP$_2$ (52).

Mutations in the PH domain that decrease binding of the N terminus of Arf1 also decrease the effect of the full-length ASAP1 on actin remodeling

ASAP1 regulates actin remodeling in cells. One GAP-dependent function is reduction of the formation of circular dorsal ruffles (CDRs) in fibroblasts treated with platelet-derived growth factor (PDGF) (4). If binding of the N terminus of Arf to the PH domain of ASAP1 were important to function, we would predict mutants with reduced binding would be less active in cells. We determined the effect of ectopic expression of WT ASAP1, [R497K]ASAP1 (a mutant with the catalytic arginine changed to lysine, which has less than 1/10,000th the activity of WT ASAP1 (4, 15)), [G339I]ASAP1 and [I423A]ASAP1. As reported previously, WT ASAP1 reduced the number of cells with CDRs. [R497K]ASAP1 did not decrease the number of cells with CDRs. [G339I]ASAP1 and [I423A]ASAP1 had an intermediate effect on CDR formation, which correlated with reduced binding to the N terminus of Arf1 and a reduction in GAP activity (Fig. 9). These results indicate the interaction between the PH domain of ASAP1 and the N terminus of Arf1 is critical for the cellular functions of ASAP1.

Discussion

We examined the mechanism by which PIP$_2$ binding to the PH domain of ASAP1 modulates activity of the GAP domain. In previous studies, we found that both the cognate PH domain of ASAP1 and the N-terminal 16 amino acids of Arf were necessary for PIP$_2$-stimulated GAP activity. Here, we report that (i) one mechanism by which the PH domain regulates GAP activity is independent of recruitment to membranes, (ii) PIP$_2$ binds to the PH domain to regulate binding to the N terminus of the substrate Arf1·GTP, and (iii) disrupting the Arf1 N terminus–PH domain association reduces GAP activity. Mutations that reduced binding of the N terminus of Arf1 to ASAP1 also reduced the activity of ASAP1 in cells. The results are consistent with our hypothesis that PIP$_2$ regulates binding of the N terminus of Arf1 to the PH domain of ASAP1, which might underlie the high degree of regulation of the catalytic activity.

The PH domain of ASAP1 contributes to enzymatic activity primarily by one of the three distinct mechanisms that have been described for PH domains. The first mechanism we had investigated was recruitment to a membrane containing a target protein (20). Our previous studies had established that recruitment was not sufficient (16, 17), and our results examining the effect of diC8PIP$_2$ and comparing the activity of [325–724]ASAP1 with [339–724]ASAP1 reported here are additional evidence that recruitment is not the primary mechanism by which ASAP1 is activated by PIP$_2$. PH domains have also been found to position autoinhibitory motifs in Grp1 and Akt such that deletion of the PH domain increases activity (37, 39). Similarly, the PH domain in SOS1 occludes the DH domain (41), the PH domain of p63RhoGEF autoinhibits the DH domain (36), and two PH domains occlude the active site in the nucleotide exchange factor Farp2 (40). Autoinhibition is relieved by Gα_q binding to a C-terminal extension of the PH domain of p63RhoGEF (36) and Arf6 binding to the PH domain and N- and C-terminal linkers on the PH domain of cytohesin (29, 39, 42). For ASAP1, deletion of the PH domain results in loss of activity (17), leading us to conclude that autoinhibition by the PH domain is not a feature of the regulation of ASAP1. Our results indicate that the PH domain of ASAP1 contributes by a third mechanism by which PH domains can affect an adjacent enzymatic domain by directly interacting with the substrate of the catalytic domain. PIP$_2$ binding to two sites within the PH domain of ASAP1 (14) is necessary for activa-

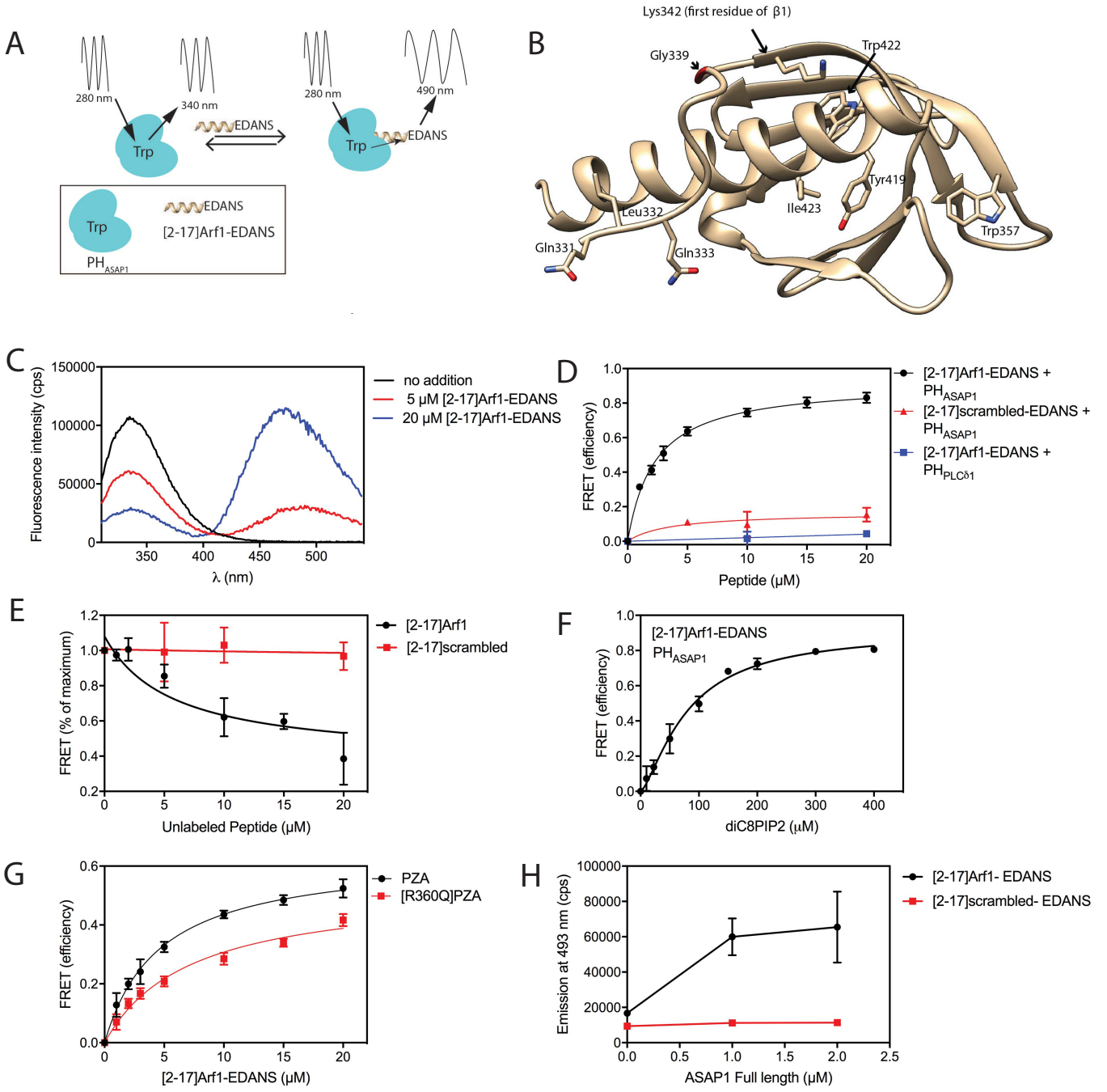

Figure 4. PIP$_2$-dependent binding of the N-terminal 16 amino acids of Arf1 to the PH domain of ASAP1 detected by FRET. *A,* principle of FRET. Nonemissive transfer of energy occurs between fluorophores with overlapping emission and excitation spectra dependent on $1/d^6$, where d is the distance between the fluorophores. Consequently, FRET occurs over short distances, such as those achieved with intermolecular association. The FRET pair used in these experiments was the tryptophans in the PH domain, with an emission peak of ~340, and EDANS, a fluorophore with an excitation peak at about 336 nm and emission at 493 nm. *B,* structure of the ASAP1 PH domain. The *ribbon structure* of the ASAP1 PH domain is shown. Side chains of tryptophans 357 and 422 are shown. Lysine 342, the first residue of the β1 strand of the PH domain, is indicated as well as residues that were changed for experiments presented in Fig. 5. The image was rendered with Chimera (90), PDB code 5C6R. *C,* representative emission spectra of PH$_{ASAP1}$ with [2–17]Arf1-EDANS. Emission spectra of 1 μM PH$_{ASAP1}$ in 200 μM diC8PIP$_2$ and the indicated concentration of [2–17]Arf1-EDANS after excitation with 280 nm light. *D,* [2–17]Arf1-EDANS dependence of FRET efficiency. 1 μM PH$_{ASAP1}$ or PH$_{PLCδ1}$ was mixed with 200 μM diC8PIP$_2$ and the indicated concentrations of [2–17]Arf1-EDANS or [2–17]scrambled-EDANS. Emission spectra were measured as in *C,* and FRET efficiency was calculated from quenching of tryptophan fluorescence as described under "Experimental procedures." FRET was quantified from quenching of tryptophan fluorescence. The results are the summary of three independent experiments and plotted as the mean ± S.E. *E,* unlabeled [2–17]Arf1 reduces FRET signal of [2–17]Arf1-EDANS. FRET was determined for 1 μM PH$_{ASAP1}$, 4 μM [2–17]Arf1-EDANS, and the indicated concentration of [2–17]Arf1 without EDANS. FRET was quantified from quenching of tryptophan fluorescence. Summary of three experiments is shown. Data are plotted as the mean ± S.E. *F,* PIP$_2$ dependence of [2–17]Arf1-PH domain binding measured by FRET. FRET was determined for a mixture of 1 μM PH$_{ASAP1}$, 15 μM [2–17]Arf1-EDANS, and the indicated concentration of diC8PIP$_2$. Summary of three experiments is shown. *G,* FRET signal requires an intact PIP$_2$-binding site. FRET, calculated as described under "Experimental procedures," was determined for a solution containing 1 μM PZA or [R360Q]PZA and the indicated concentrations of [2–17]Arf1-EDANS. Summary of three experiments is shown. *H,* [2–17]Arf1 binding to full-length ASAP1. Full-length ASAP1 was titrated into a mixture containing 2 μM [2–17]Arf1-EDANS or [2–17]scrambled-EDANS, as indicated, and 200 μM diC8PIP$_2$. Samples were excited with 280 nm light. Emission at 493 is shown. Summary of two experiments is shown. Data are plotted as the mean ± S.E.

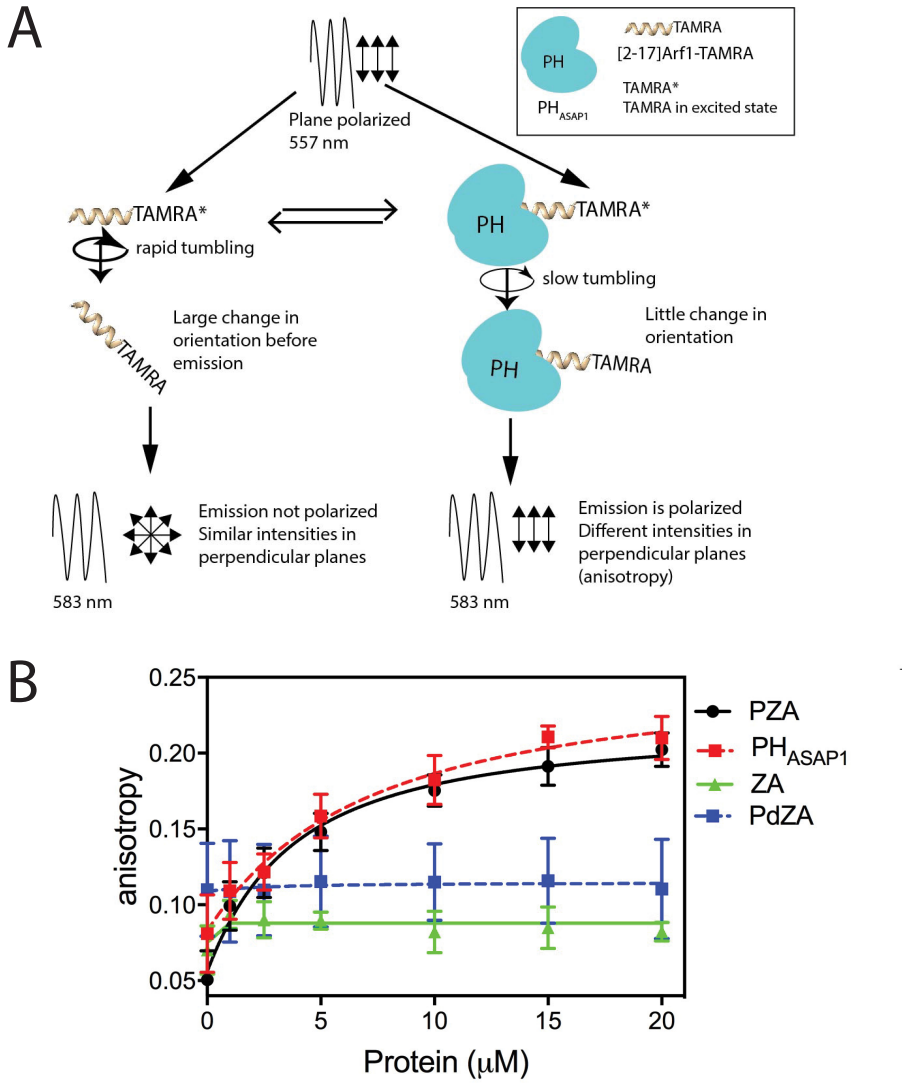

Figure 5. [2–17]Arf1–ASAP1 association is specific for PH$_{ASAP1}$ as measured by fluorescence anisotropy. *A,* principle of fluorescence anisotropy. A molecule with a linked fluorophore is excited with plane polarized light. If the molecule tumbles rapidly, relative to the lifetime of the excited fluorophore such that the fluorophore randomly changes its orientation before emission, the emission is depolarized and intensity in perpendicular planes is similar. If the molecule tumbles slowly, *e.g.* as would occur if it binds to a larger molecule, the emission will be partly polarized, with unequal intensities in perpendicular planes, which is a measure of anisotropy. *B,* fluorescence anisotropy of TAMRA linked to [2–17]Arf1 is increased by incubation with the ASAP1 PH domain. Fluorescence anisotropy of 1 μM [2–17]Arf1-TAMRA in a mixture containing 200 μM diC8PIP$_2$ and the indicated protein at the indicated concentration was determined. Summary of three experiments is shown and plotted as the mean ± S.E.

tion, in part by recruiting the ASAP1 to a surface containing Arf1, but largely through an effect on the PH domain that facilitates binding to the N terminus of Arf1.

The association of the ASAP1 PH domain with the substrate for the GAP domain, Arf1, has some features in common with other proteins with PH domains that regulate small GTP-binding proteins. A PH domain binding a substrate to contribute to catalysis was first reported for DH–PH domain proteins. The PH domain of Dbs binds to switch 2 and helix α3b of Rac1 to promote exchange of nucleotides (62). For Brag2, an Arf-exchange factor, switch 1 of Arf binds to an expansion of the PH domain, formed by the linker between sec7 and the PH domain (43). ASAP1 is distinct from these in that the PH domain binds to the N-terminal extension of Arf1.

Like the PH domains of cytohesins, the ASAP1 PH domain binds to Arf under the control of PIP$_2$ (29, 39, 42), but the mechanism is distinct. Switch 1, the interswitch domain, and switch 2 contribute to binding to the PH domain of the cytohesin Grp1. In contrast, the N terminus of Arf binds to the PH domain of ASAP1, although we cannot exclude some involvement of switch 1 or 2. Another difference is that binding to the cytohesin PH domain is driven by binding a single phosphoinositide molecule. For ASAP1, simultaneous binding of two phospholipids to a single PH domain is necessary. A third difference is that Arf binding to the PH domain of cytohesin 3 (Grp1) involves linkers on both the N- and C-terminal regions of the PH domain. Although there is some contribution of an interdomain linker, the linker is not required for binding between the ASAP1 PH domain and Arf1.

We investigated the role of a 17-amino acid extension of the PH domain based on the precedent of cytohesins (29, 39, 42)

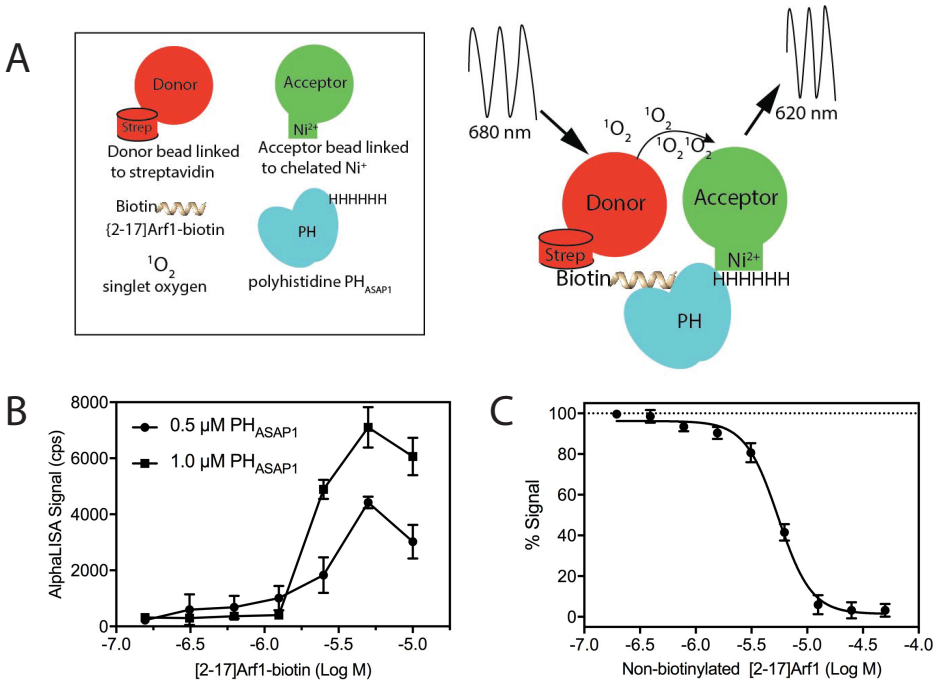

Figure 6. [2–17]Arf1–PH$_{ASAP1}$ association detected by an AlphaScreen® assay. *A,* principle of the AlphaLISA® assay. Biotinylated [2–17]Arf1 and the His-tagged PH domain were mixed with a donor bead derivatized with streptavidin and acceptor beads derivatized with chelated Ni^{2+}. The donor beads bound to the biotin on [2–17]Arf1 and released singlet oxygen on excitation with 680 nm light. The acceptor beads bound to the His tag of the PH domain and emitted 620 nm light if near the source of singlet oxygen. Binding of the PH domain to [2–17]Arf1 would bring the beads close enough for efficient delivery of the singlet oxygen generated by the donor beads to the acceptor beads to give a 620 nm emission signal. *B,* AlphaScreen® signal is proportional to the PH domain concentration. Interactions of 0.5 or 1 μM PH$_{ASAP1}$ with a range of [2–17]Arf1-biotin concentrations were evaluated by the AlphaScreen® assay. The largest dynamic range is obtained with 5 μM peptide, above which the signal decreases due to the "hook effect" (60). The data are shown as mean values ± S.D. of four technical replicates. *C,* affinity of [2–17]Arf1 for PH$_{ASAP1}$ evaluated by competition with the unlabeled peptide. The nonbiotinylated [2–17]Arf1 peptide inhibits the interaction between 1 μM PH$_{ASAP1}$ and 5 μM [2–17]Arf1-biotin (IC_{50} = 5.4 μM; Hill slope = −2.8). The data are shown as mean values ± S.D. of four technical replicates and fit to a nonlinear four-parameter equation.

and p63RhoGEF (36). For cytohesins, linkers N- and C-terminal to the PH domain are critical for binding Arf6. For p63RhoGEF, a C-terminal extension of the PH domain mediates binding to Gα_q. We found that the 17-amino acid N-terminal extension of the PH domain had a minimal contribution to binding the N terminus of Arf1 but was nevertheless critical for GAP activity, independent of both PIP_2 binding and peptide binding. This result provides additional support for the notion that the PH domain is not simply a recruitment mechanism as the PH domain without the linker was recruited to LUVs by PIP_2 nearly as well as the PH domain with the linker, but PZA without the linker had a fraction of the activity of PZA containing the linker. In addition, the results indicate that there is a difference in regulation of GAP activity by PIP_2 in a membrane compared with a soluble analog of PIP_2, with a larger differential in activity with and without the linker observed with LUVs than with diC8PIP_2. Possible mechanisms by which the N-terminal extension of the PH domain affects the GAP domain and how this is influenced by a lipid bilayer are currently being explored.

Other PH domains bind to protein and phospholipids simultaneously but cooperativity similar to that seen in cytohesin and ASAP1 has not been reported. One example is the phosphotyrosine binding (PTB) domain[11] of disabled-1 (Dab1), which binds simultaneously to PIP_2 and peptides containing Asn–Pro–Xaa–Tyr found in, for example, amyloid precursor protein and the apolipoprotein E receptor 2 (64, 65). Dab1 binds to PIP_2 through a site that aligns with the PIP_2-binding site of the PH domain of PLC δ1. The peptide-binding site is separate and involves the β5-strand and the C-terminal α-helix. Other than by restricting the protein to the cellular site with the target peptide, PIP_2 does not influence peptide binding (65). Another example of a PH domain that binds simultaneously to a phosphoinositide and protein is the PH domain of FAPP1 (Four-phosphate-adaptor protein 1), which binds to Arf1 and phosphatidylinositol 4-phosphate simultaneously (26, 27). Both ligands are on the same surface, which allows coincidence detection; however, we are not aware of evidence for cooperative binding.

The proposed function of the ASAP1 PH domain is similar to models for GTPases (66, 67). For both, ligand binding (phosphoinositides or guanine nucleotides) controls the affinity for a target protein. The important difference between PH domains and GTPases is related to the mechanisms for switching between active and inactive conformations. For GTPases, high-affinity binding of nucleotide rapidly activates the protein, whereas rapid inactivation is achieved by a catalytic event, GTP hydrolysis. PH domains do not have a catalytic activity to rapidly convert to the inactive form. The conversion from inactive to active and back is

[11] PH, PTB, EVH1, and RanBD have a common fold, referred to as the PH domain superfold (63).

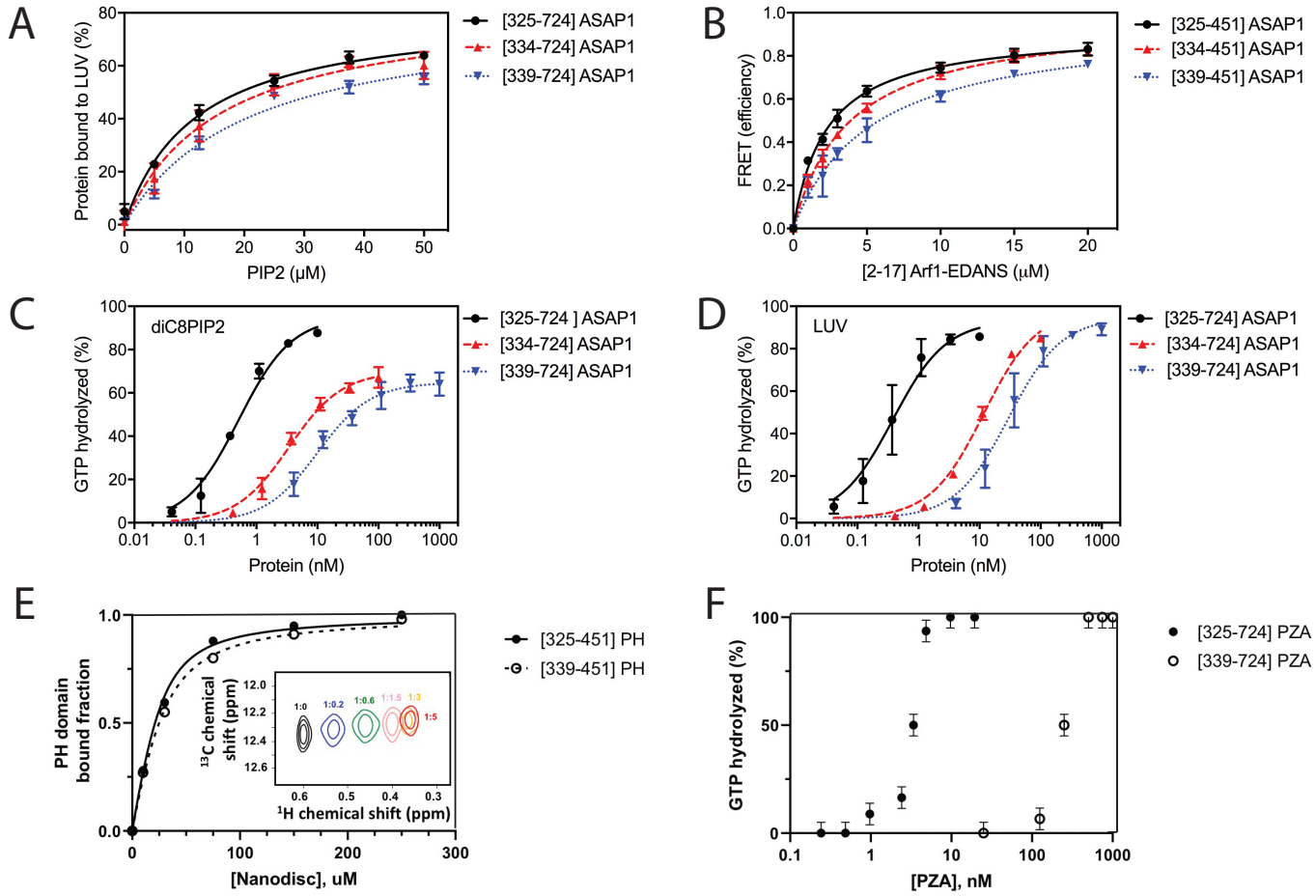

Figure 7. Effects of the N-terminal extension (residues 325–339) of the PH domain on peptide and PIP$_2$ binding and GAP activity. *A,* binding of the PH domain to PIP$_2$ in LUVs. Sucrose-LUVs, with a total phospholipid concentration of 500 μM containing 75 μM PS and the indicated concentration of PIP$_2$, were incubated with the indicated recombinant proteins and removed from bulk solution by centrifugation. Protein that precipitated with the LUVs was fractionated by SDS-PAGE, visualized with GEL-CODE Blue stain (Thermo Fisher Scientific), and quantified by scanning densitometry. The results presented are the summary of three independent experiments plotted as means ± S.E. *B,* PH domain binding to [2–17]Arf1. Binding of the indicated recombinant PH domain of ASAP1 to [2–17]Arf1 was measured by FRET as described in Fig. 3. The summary of three independent experiments is presented. *C,* GAP activity with diC8PIP$_2$. The indicated proteins were titrated into a reaction mixture containing 200 μM diC8P2 and 0.1 μM [L8K]Arf1·GTP. GAP activity was measured as described in Fig. 1 and under "Experimental procedures." Results shown are the summary of three experiments. *D,* GAP activity with LUVs. The indicated proteins were titrated into reaction mixtures with LUVs containing 15% PS, 5% PIP$_2$ at a total phospholipid concentration of 500 and 0.1 μM myrArf1·GTP. GAP activity was determined as in *C*. The summary of three experiments is shown. *E,* evaluation of binding of the ASAP1 PH domain to nanodiscs by NMR. Nanodiscs were titrated into a solution containing the indicated [^{13}C]methyl-labeled PH domain, and chemical shift perturbations were followed. *Inset,* 2D ^{1}H-^{13}C HMQC spectra of Ile-371 with increasing concentrations of nanodiscs. *F,* GAP activity in nanodiscs. The indicated proteins were titrated into a reaction containing 5 μM myrArf1·GTP as a substrate. The total concentration of exposed lipids was 500 μM. The percentage of GTP bound to myr-Arf1 hydrolyzed in 3 min is plotted against protein concentration.

controlled by ligand binding and dissociation. Cooperative binding of phospholipids, as reported for ASAP1 (14), may provide rapid allosteric regulation of activity.

Our results highlight the possible importance of extensions from the nucleotide-binding domain for signaling in Ras-superfamily proteins. A role of an extension from the nucleotide-binding domain for protein function was described as early as 1991 for Arf family proteins. In Arf, the N-terminal extension from the nucleotide-binding fold (68) is myristoylated and associates with membranes when Arf is bound to GTP. Arf1 without the extension was found to be inactive *in vitro* and in cell-based functional assays (69, 70). A peptide composed of these 16 amino acids of Arf1 blocked *in vitro* assays of Arf activity (69, 71). Several years later, the finding of relative movement of the Arf1 N terminus on GTP binding supported the idea that it functioned as a third switch motif in Arf (50, 72). Here, we observe that it binds directly to the GAP, which promotes GAP activity. Efficient interaction of Arf with the exchange factor Brag2 might also involve the N terminus of Arf (43, 73). Extensions of other G proteins from the GTPase domain have been found to bind effector proteins. Most relevant for Arf is Arl2 in which the N-terminal helix, switch 1, and switch 2 are all part of the interface with Binder of Arl Two (BART) (74). The C-terminal hypervariable region (HVR), an extension of the nucleotide binding fold, of other Ras superfamily members might be similarly important. In molecular dynamic simulations coupled with FRET measurements in living cells, the accessibility of the HVR of Ras was determined by the bound nucleotide (75–77). In other studies, Rheb and KRas4b were reported to bind phosphodiesterase through the HVR with no contact with switch 1 or 2 (78, 79).

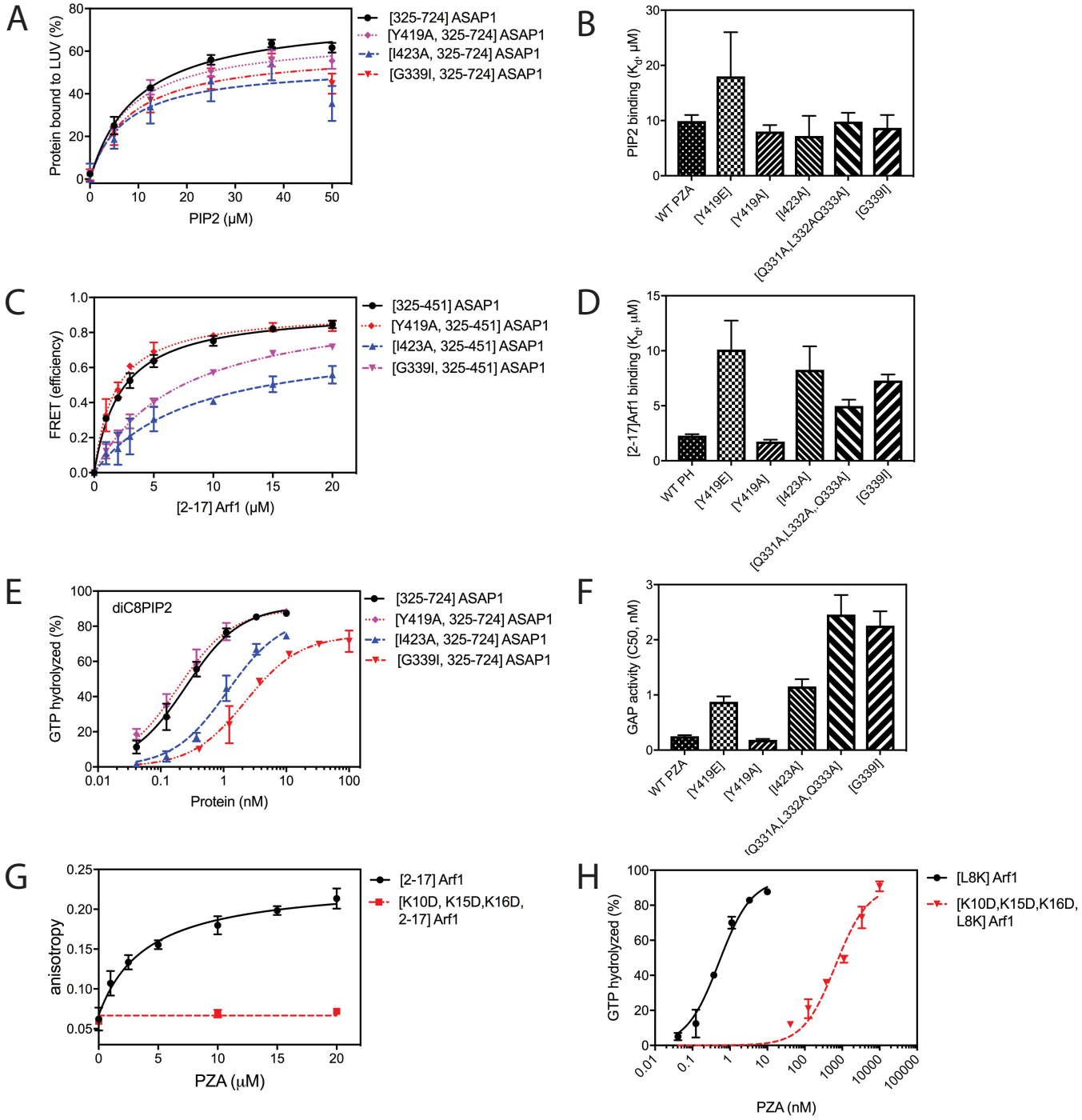

Figure 8. Correlation of effects of mutations in the PH domain and the N terminus of Arf1 on [2–17]Arf1-PH domain association and GAP activity. *A–F*, mutations in the PH domain. Residues in the N-terminal extension of the PH domain and the C-terminal α-helix were changed as indicated (see Fig. 4*A*). *A* and *B*, effect on binding to PIP_2 in LUVs. Binding of the indicated proteins to LUVs with the indicated concentrations of PIP_2 was measured as described in Fig. 4*C* and under "Experimental procedures." *A*, binding isotherms for four proteins are shown. *B*, K_d values, estimated from the isotherms, are presented. *C* and *D*, effect on [2–17]Arf1 binding. Binding of [2–17]Arf1 to the indicated proteins was measured by FRET as described in Fig. 3 and under "Experimental procedures." *C*, binding isotherms of four proteins are shown. *D*, dissociation constants (K_d values) determined from the binding isotherms are shown. *E* and *F*, effect on GAP activity. The indicated proteins were titrated into a reaction containing 0.1 μM [L8K]Arf1·GTP and 200 μM diC8PIP_2. *E*, dependence of GTP hydrolysis on protein concentration is shown. *F*, C_{50} values, estimated from the concentration dependence, are presented. *G*, effect of mutating lysines 10, 15, and 16 of Arf on binding to the ASAP1. Fluorescence anisotropy of 1 μM [2–17]Arf1-TAMRA or [K10D,K15D,K16D (*KK15,16DD*), 2–17]Arf-TAMRA in a mixture containing 200 μM diC8PIP_2 and the indicated concentration of PZA was determined. *H*, effect of mutations in the N terminus of Arf1 on GAP activity. PZA was titrated into a reaction containing 200 μM diC8PIP_2 and either [L8K]Arf1·GTP or [L8K,K10D,K15D,K16D]Arf1·GTP. The summary of three experiments is shown and presented as means ± S.E.

In summary, our results support the hypothesis that PIP_2-dependent binding of the N terminus of Arf1 to the PH domain of ASAP1 regulates GAP activity. In ongoing studies, we will continue to test the hypothesis with full-length ASAP1 in cells and will identify the binding interface and the mechanism by which PIP_2 binding to the PH domain facilitates the interaction.

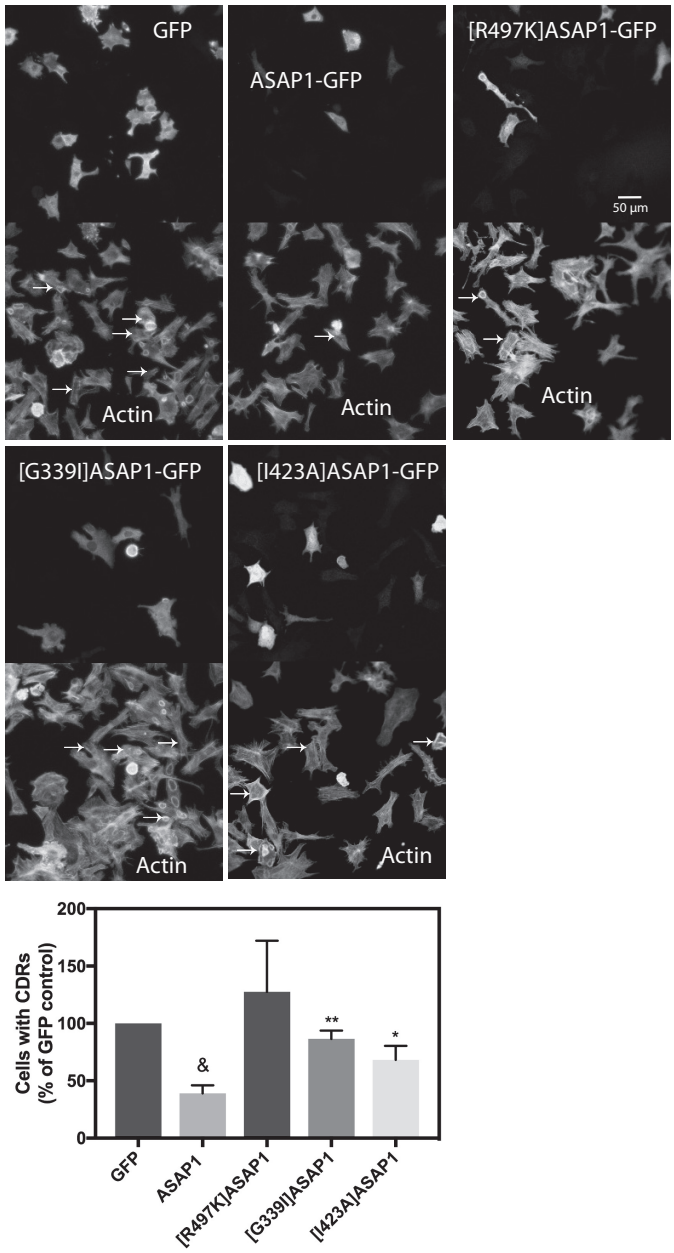

Figure 9. Mutations in the PH domain of ASAP1 that reduce binding to the N terminus of Arf1 also reduce effect of ASAP1 on circular dorsal ruffles in cells. CDRs were induced in NIH 3T3 fibroblasts transfected with plasmids for expression of the indicated proteins by treatment with PDGF. The number of transfected cells containing CDRs and the total number of transfected cells were determined by manual counting. Representative images for each of the conditions are shown. *Arrows* point to cells with CDRs. The ratio of cells forming CDRs under each condition to the control cells, presented as a percentage, was used to summarize the data for four experiments with all conditions except [R497K]ASAP1, which was examined in two experiments (46 ± 10% of control cells (expressing GFP) had CDRs). *Error bars* are S.E. *, $p <$ 0.05; **, $p < 0.01$ compared with WT ASAP1; &, $p < 0.05$ compared with GFP-transfected control, based on paired *t* tests calculated using GraphPad Prism.

Experimental procedures

Materials

The following peptides were purchased from Lifetein, Hillsborough, NJ: 1) [2–17]Arf1, sequence GNIFANLFKGLFGKKE; 2) [2–17]scrambled, sequence AKLGKLGKFNNGIFFE; 3) [2–17]Arf1-TAMRA, sequence GNIFANLFKGLFGKKE-K(TAMRA); 4) [K10D, K15D, K16D, 2–17]; 5) [2–17]Arf1-EDANS, sequence GNIFANLFKGLFGKKE-E(EDANS); 6) [2–17]scrambled-EDANS, sequence AKLGKLGKFNNGIFFE-E(EDANS); 7) [2–17]Arf1-biotin, sequence GNIFANLFKGLFGKKEK(Biotin). [α^{32}P]GTP was purchased from PerkinElmer Life Sciences; PEI-cellulose plates were from Selecto Scientific; nitrocellulose filters, 25-mm circles, BA85, were from GE Healthcare; Nucleopore Track-Etch membranes were from Whatman. The following lipids were from Avanti Polar Lipids: phosphatidylcholine; phosphatidylethanolamine; PS; cholesterol, phosphatidylinositol;, phosphatidylinositol 4,5-bisphosphate; 1-palmitoyl-2-oleoyl-*sn*-glycero-3-phosphocholine; and 1-oleoyl-2-oleoyl-*sn*-phosphatidylinositol 4,5-bisphosphate. The following lipid analogs were from Echelon Biosciences and Cayman Chemicals: 1,2-dibutanoyl-PIP$_2$; sodium salt (diC4PIP$_2$); (1,2 dihexanoyl-PIP$_2$; sodium salt (diC6PIP$_2$); 1,2-dioctanoyl-PIP$_2$; sodium salt (diC8PIP$_2$).

Lipofectamine LTX with Plus reagent were purchased from Thermo Fisher Scientific. Fibronectin and recombinant human PDGF BB were purchased from Sigma.

Alexa Fluor 594 phalloidin (A12381), GFP rabbit polyclonal antibody (A6455), and anti-rabbit secondary antibody Alexa Fluor 488 (A21206) were from Invitrogen. Dako fluorescence mounting medium was purchased from Agilent.

Protein expression and purification

Bacterial expression vectors for polyhistidine-tagged [325–724]ASAP1 (ASAP1 PZA), polyhistidine-tagged [325–451]ASAP1 (PH$_{ASAP1}$), polyhistidine-tagged [441–724]ASAP1 (ZA), [1–134]PLCδ1 (PH$_{PLCδ1}$), the chimeric protein composed of [1–134]PLCδ1 fused to [441–724]ASAP1 (PdZA), Arf1, [L8K]Arf1, and [Δ17]Arf1 have been previously described (15–17). Expression vectors for polyhistidine-tagged [334–451]ASAP1, [339–451]ASAP1, [334–724]ASAP1, and [339–724]ASAP1 were prepared by PCR amplification of the ORF and inserting the ORF into pET19 in the Nde/EcoRI sites. Expression vectors for polyhistidine-tagged [Y419A,325–451]ASAP1, [Y419E,325–451]ASAP1, [I423A,325–451]ASAP1, [Q331A,L332A,Q333A,325–451]ASAP1, [G339I,325–451]ASAP1, [Y419A,325–724]ASAP1, [Y419E,325–724]ASAP1, [I423A,325–724]ASAP1, [Q331A,L332A,Q333A,325–451]ASAP1, [325–724]ASAP1, and [G339I,325–724]ASAP1 were prepared using the QuikChange site-directed mutagenesis kit (Agilent). Recombinant proteins were expressed and purified from bacteria as described (17, 80, 81). Full-length ASAP1 with a C-terminal hexahistidine tag was expressed in Sf9 cells using a baculovirus expression system and purified on a His trap column followed by size exclusion on Sephacryl S-300. The plasmid for expressing ASAP1b-GFP in mammalian cells, which included a 37-amino acid linker (NLSSDSSLSSPSALNSLSSPSALNSTASNSPGIEGLS) at the C terminus of mouse ASAP1b, was generated by PCR. The insert was cloned into pEGFP-N2 using 5′-XhoI and 3′-EcoRI restriction sites. The G339I, I423A, and R497K mutants of ASAP1b-GFP were generated using the QuikChange site-directed mutagenesis kit (Agilent) with the WT construct as template.

Preparation of LUVs

LUVs were prepared by lipid extrusion. Lipids in chloroform solution were mixed in a siliconized glass 12 × 17-mm tube at the indicated molar ratios with a total lipid mass of 0.5 to 2.5

μmol. Chloroform was removed by streaming nitrogen over the solution for 1 h and then placing the tubes in a lyophilizer for an additional hour. Lipids were hydrated with 0.1 to 0.5 ml (volume for final lipid concentration of 5 mM total lipid) of 25 mM HEPES, pH 7.4, 100 mM NaCl, 1 mM DTT, with or without 10% sucrose (w/v) as indicated, and then subjected to five freeze–thaw cycles followed by extrusion through Whatman Nuclepore Track-etched membranes, with 1-μm pores, in an Avanti Polar Lipids lipid extruder (82).

GAP assays

GAP activity was determined by measuring the conversion of [α-^{32}P]GTP bound to Arf1 to [α-^{32}P]GDP as described (80). For experiments in which the GAP was titrated into a reaction, the concentration of GAP required to induce hydrolysis of 50% of the bound GTP in 3 min is referred to as the C_{50}. For experiments with a fixed concentration of GAP, activity was expressed as $\ln(S_0/S)/t$ in which S_0 is the initial amount of substrate, Arf·GTP, and S is the amount of substrate remaining after a fixed time, *t*, which was typically 3 min (48).

GAP activity was also determined by following the reduction in tryptophan fluorescence that is observed when Arf·GTP is converted to Arf·GTP as described (83–85). In these experiments, [325–724]ASAP1 or [339–724]ASAP1 was titrated into a reaction containing myrArf1·GTP bound to nanodiscs (NDs). The tryptophans were excited at 297 nm, and emission at 340 nm was measured.

FRET

Peptides were labeled with EDANS either at the C or N terminus through an extra glutamic acid. EDANS-labeled peptides and protein were incubated in PBS, pH 7.4, with further additions as indicated in the figure legends and text. The samples were excited at 280 nm and emission spectra recorded from 310 to 540 nm with a Jobin-Yvon Horiba FluroMax-3 spectrofluorimeter. Excitation and emission slit widths were 5 nm. For experiments in which the peptide was titrated, FRET efficiency (*E*) was calculated from the intensities at 340 nm using Equation 1,

$$E = 1 - \frac{F_{da}}{F_d} \quad \text{(Eq. 1)}$$

where F_{da} is the intensity in presence of acceptor and F_d is the intensity without acceptor.

In experiments in which the donor (protein) was titrated, emission from the acceptor to shown as a measure of FRET.

Fluorescence anisotropy

Proteins were titrated into a reaction containing 1 μM [2–17]Arf1-Lys-TAMRA or 1 μM [2–17]scrambled-Lys-TAMRA and 200 μM diC8PIP$_2$ in PBS, pH 7.4. Fluorescence anisotropy was measured at 30 °C using a PerkinElmer Life Sciences LS55, with an excitation wavelength of 557 nm and emission wavelength of 583 nm and 5-nm slit widths. The steady-state fluorescence anisotropy (*A*) was calculated according to Equation 2,

$$A = \frac{I_{\parallel} - G \times I_{\perp}}{I_{\parallel} + 2G \times I_{\perp}} \quad \text{(Eq. 2)}$$

where $I_{\parallel}$ is the parallel emission intensity, $I_{\perp}$ is the perpendicular emission intensity, and *G* is the grating factor that corrects for wavelength-dependent distortion of the polarizing system (59, 86). Titrations were repeated at least three times. The average anisotropy value for each concentration of protein was fit to a single-site binding equation in GraphPad Prism to calculate the dissociation constant, K_d.

AlphaScreen® assay

A solution containing 266.7 μM diC8PIP$_2$ with 1.3-fold the indicated concentrations of [2–17]Arf1-biotin and PH$_{ASAP1}$ in 50 mM Tris-HCl, 100 mM NaCl, pH 8.68, was dispensed as 3-μl volumes into the wells of a white, solid bottom 1,536-well plate (Greiner, catalog no. 789175-F). For the competition analysis, nonbiotinylated [2–17]Arf1 peptide was prepared in DMSO as a 15-point concentration series with 2-fold dilution and pin-transferred (20 nl) to the assay plate by a Kalypsys pin-tool equipped with a 1,536-pin array, resulting in a final peptide concentration range of 3 nM to 50 μM. After a 60-min incubation at room temperature, 1 μl containing 80 μg/ml nickel chelate acceptor beads (20 μg/ml, final) and 80 μg/ml streptavidin donor beads (20 μg/ml, final) (AlphaScreen® histidine (nickel chelate) detection kit, catalog no. 6760619R, PerkinElmer Life Sciences) was dispensed into each well and allowed to incubate for 60 min at room temperature in the dark. The AlphaScreen® signal was read by a PerkinElmer Life Sciences EnVision plate reader with an ultrasensitive luminescence detector and 1,536 plate HTS AlphaScreen® aperture (excitation of 680 nm and emission of 615 nm).

Analysis of chemical cross-linking of [2–17]Arf1 to PH$_{ASAP1}$

20 μM [2–17]Arf1-TAMRA and 20 μM PH$_{ASAP1}$ were mixed in the presence of 500 μM sucrose-loaded LUV with 2.5% PIP$_2$ and 15% PS in 100 mM Mes, pH 6.0, 150 mM NaCl. After 20 min, EDC was added to a final concentration of 600 μM. The mixture was incubated for 2 h at 25 °C with shaking. The reaction was quenched with 4 mM β-mercaptoethanol. The pH of the reaction was adjusted to 7 by addition of Tris, pH 8. The sample was treated with trypsin followed by centrifugation to precipitate the LUVs. Mass spectra of the trypsin-treated supernatants were collected with an Orbitrap Fusion mass spectrometer, and data were analyzed with pLink software (87, 88).

Preparation of membrane scaffolding protein (MSP) belt proteins

The plasmids for MSPΔH5 were the generous gift of Drs. Franz Hagn and Gerhard Wagner (Harvard Medical School) to Dr. Byrd. The proteins were expressed and purified as described previously (89).

Preparation of NDs

Lipids were mixed in chloroform solutions, then air-dried with nitrogen flow, and re-solubilized with cholate in aqueous buffer (20 mM Tris-HCl, pH 7.4, 150 mM NaCl, and 75 mM sodium cholate). NDs were prepared using 1-palmitoyl-2-oleoyl-*sn*-glycero-3-phosphocholine and 1-oleoyl-2-oleoyl-*sn*-phosphatidylinositol 4,5-bisphosphate. NDs were assembled by mixing MSPΔH5 with solubilized lipids at a 1:45 ratio, followed by removal of sodium cholate from the mixture with Bio-Beads

SM-2 (Bio-Rad). Assembled NDs were then purified via a Superdex-200 size-exclusion column (GE Healthcare).

NMR measurements and chemical shift perturbation analysis

All NMR spectra were collected at 25 °C on a Bruker Avance III 850 MHz spectrometer equipped with TCI triple-resonance cryoprobes. Chemical shift perturbations were analyzed by Equation 3,

$$\Delta\delta_{obs} = \Delta\delta_{max} \cdot [((n \cdot P_t) + L_t + k_d) - [(n \cdot P_t) + L_t + k_d)^2 - 4 \cdot (n \cdot P_t) \cdot (L_t)]^{1/2}]/2 \cdot n \cdot P_t \quad \text{(Eq. 3)}$$

where $\Delta\delta_{obs}$, $\Delta\delta_{max}$, P_t, L_t, and k_d values are the change in the observed chemical shift from the free state, the maximum change in chemical shift, the total PH domain concentration, the concentration of ND, and the dissociation constant, respectively. Data converged to n, the number of sites, equal to 2, indicating that a nanodisc can bind one PH domain on each of its sides.

Cell biology

NIH 3T3 clone 7, kindly provided by Dr. Douglas Lowy, was maintained in Dulbecco's modified Eagle's medium with 10% fetal bovine serum and 1× penicillin/streptomycin. Cells were transfected with 2.5 μg/ml plasmids for expression of GFP or the indicated ASAP1 protein fused to GFP with Lipofectamine LTX Plus reagent and used 24 h later. CDRs were induced in cells plated on 10 μg/ml fibronectin-coated coverslips that were maintained for 5 h in Opti-MEM with no serum by treating with 20 ng/ml PDGF for 5 min. Cells were fixed with 4% paraformaldehyde. Before staining for immunofluorescence, cells were permeabilized with 0.2% saponin, 0.5% BSA, and 1% fetal bovine serum in PBS. Actin in the CDRs was stained with Alexa 594 phalloidin, and ASAP1–GFP or GFP was visualized using primary GFP rabbit polyclonal antibody followed by the anti-rabbit secondary antibody conjugated to Alexa Fluor 488. Mounting was done using Dako fluorescence mounting medium. Microscope images were captured using a Leica SP8 laser-scanning confocal microscope using a ×20, 0.75 numerical aperture objective (Leica Microsystems Inc, Buffalo Grove, IL). Single slices were collected with the pinhole size set to 6.28 airy units. At least 25 cells were counted for each condition for each of four experiments (two for [R497K]ASAP1).

Author contributions—N. S. R., O. S., N. P. C., M. D. H., M. E. Y., and P. A. R. conceptualization; N. S. R., O. S., and P. A. R. data curation; N. S. R., O. S., L. M. J., R. A. B., and P. A. R. formal analysis; N. S. R., X. J., O. S., P. Z., J. R. H., J. N. D., N. P. C., L. M. J., R. L., I. O. A., and M. E. Y. investigation; N. S. R., X. J., O. S., N. P. C., L. M. J., M. D. H., M. E. Y., and P. A. R. writing-review and editing; O. S., N. P. C., L. M. J., M. E. Y., and P. A. R. methodology; M. D. H., R. A. B., M. E. Y., and P. A. R. resources; M. D. H., R. A. B., M. E. Y., and P. A. R. supervision; M. D. H., M. E. Y., and P. A. R. project administration; M. E. Y. and P. A. R. writing-original draft.

Acknowledgments—We thank Kate Hebron for insightful discussions, Douglas Lowy for Clone 7 NIH 3T3 fibroblasts, and Valerie Barr for help with microscopy. Molecular graphics were performed with UCSF Chimera, developed by the Resource for Biocomputing, Visualization, and Informatics at the University of California, San Francisco, with support from National Institutes of Health Grant P41-GM103311.

References

1. Kahn, R. A., Bruford, E., Inoue, H., Logsdon, J. M., Jr., Nie, Z., Premont, R. T., Randazzo, P. A., Satake, M., Theibert, A. B., Zapp, M. L., and Cassel, D. (2008) Consensus nomenclature for the human ArfGAP domain-containing proteins. *J. Cell Biol.* **182,** 1039–1044 CrossRef Medline
2. Brown, M. T., Andrade, J., Radhakrishna, H., Donaldson, J. G., Cooper, J. A., and Randazzo, P. A. (1998) ASAP1, a phospholipid-dependent Arf GTPase-activating protein that associates with and is phosphorylated by Src. *Mol. Cell. Biol.* **18,** 7038–7051 CrossRef Medline
3. Bharti, S., Inoue, H., Bharti, K., Hirsch, D. S., Nie, Z., Yoon, H. Y., Artym, V., Yamada, K. M., Mueller, S. C., Barr, V. A., and Randazzo, P. A. (2007) Src-dependent phosphorylation of ASAP1 regulates podosomes. *Mol. Cell. Biol.* **27,** 8271–8283 CrossRef Medline
4. Randazzo, P. A., Andrade, J., Miura, K., Brown, M. T., Long, Y. Q., Stauffer, S., Roller, P., and Cooper, J. A. (2000) The Arf GTPase-activating protein ASAP1 regulates the actin cytoskeleton. *Proc. Natl. Acad. Sci. U.S.A.* **97,** 4011–4016 CrossRef Medline
5. Randazzo, P. A., Inoue, H., and Bharti, S. (2007) Arf GAPs as regulators of the actin cytoskeleton. *Biol. Cell* **99,** 583–600 CrossRef Medline
6. Liu, Y., Loijens, J. C., Martin, K. H., Karginov, A. V., and Parsons, J. T. (2002) The association of ASAP1, an ADP ribosylation factor-GTPase activating protein, with focal adhesion kinase contributes to the process of focal adhesion assembly. *Mol. Biol. Cell* **13,** 2147–2156 CrossRef Medline
7. Liu, Y., Yerushalmi, G. M., Grigera, P. R., and Parsons, J. T. (2005) Mislocalization or reduced expression of arf GTPase-activating protein ASAP1 inhibits cell spreading and migration by influencing Arf1 GTPase cycling. *J. Biol. Chem.* **280,** 8884–8892 CrossRef Medline
8. Ehlers, J. P., Worley, L., Onken, M. D., and Harbour, J. W. (2005) DDEF1 is located in an amplified region of chromosome 8q and is overexpressed in uveal melanoma. *Clin. Cancer Res.* **11,** 3609–3613 CrossRef Medline
9. Onodera, Y., Hashimoto, S., Hashimoto, A., Morishige, M., Mazaki, Y., Yamada, A., Ogawa, E., Adachi, M., Sakurai, T., Manabe, T., Wada, H., Matsuura, N., and Sabe, H. (2005) Expression of AMAP1, an ArfGAP, provides novel targets to inhibit breast cancer invasive activities. *EMBO J.* **24,** 963–973 CrossRef Medline
10. Buffart, T. E., Coffa, J., Hermsen, M. A., Carvalho, B., van der Sijp, J. R., Ylstra, B., Pals, G., Schouten, J. P., and Meijer, G. A. (2005) DNA copy number changes at 8q11–24 in metastasized colorectal cancer. *Cell. Oncol.* **27,** 57–65 Medline
11. Hou, T., Yang, C., Tong, C., Zhang, H., Xiao, J., and Li, J. (2014) Overexpression of ASAP1 is associated with poor prognosis in epithelial ovarian cancer. *Int. J. Clin. Exp. Pathol.* **7,** 280–287 Medline
12. Lin, D., Watahiki, A., Bayani, J., Zhang, F., Liu, L., Ling, V., Sadar, M. D., English, J., Fazli, L., So, A., Gout, P. W., Gleave, M., Squire, J. A., and Wang, Y. Z. (2008) ASAP1, a gene at 8q24, is associated with prostate cancer metastasis. *Cancer Res.* **68,** 4352–4359 CrossRef Medline
13. Müller, T., Stein, U., Poletti, A., Garzia, L., Rothley, M., Plaumann, D., Thiele, W., Bauer, M., Galasso, A., Schlag, P., Pankratz, M., Zollo, M., and Sleeman, J. P. (2010) ASAP1 promotes tumor cell motility and invasiveness, stimulates metastasis formation *in vivo*, and correlates with poor survival in colorectal cancer patients. *Oncogene* **29,** 2393–2403 CrossRef Medline
14. Jian, X., Tang, W. K., Zhai, P., Roy, N. S., Luo, R., Gruschus, J. M., Yohe, M. E., Chen, P. W., Li, Y., Byrd, R. A., Xia, D., and Randazzo, P. A. (2015) Molecular basis for cooperative binding of anionic phospholipids to the PH domain of the Arf GAP ASAP1. *Structure* **23,** 1977–1988 CrossRef Medline
15. Luo, R., Ahvazi, B., Amariei, D., Shroder, D., Burrola, B., Losert, W., and Randazzo, P. A. (2007) Kinetic analysis of GTP hydrolysis catalysed by the Arf1–GTP–ASAP1 complex. *Biochem. J.* **402,** 439–447 CrossRef Medline
16. Che, M. M., Boja, E. S., Yoon, H. Y., Gruschus, J., Jaffe, H., Stauffer, S., Schuck, P., Fales, H. M., and Randazzo, P. A. (2005) Regulation of ASAP1 by phospholipids is dependent on the interface between the PH and Arf GAP domains. *Cell. Signal.* **17,** 1276–1288 CrossRef Medline
17. Kam, J. L., Miura, K., Jackson, T. R., Gruschus, J., Roller, P., Stauffer, S., Clark, J., Aneja, R., and Randazzo, P. A. (2000) Phosphoinositide-dependent activation of the ADP-ribosylation factor GTPase-activating protein ASAP1–evidence for the pleckstrin homology domain functioning as an allosteric site. *J. Biol. Chem.* **275,** 9653–9663 CrossRef Medline

18. Balla, T. (2005) Inositol-lipid binding motifs: signal integrators through protein–lipid and protein–protein interactions. *J. Cell Sci.* **118,** 2093–2104 CrossRef Medline
19. Lemmon, M. A. (2003) Phosphoinositide recognition domains. *Traffic* **4,** 201–213 CrossRef Medline
20. Moravcevic, K., Oxley, C. L., and Lemmon, M. A. (2012) Conditional peripheral membrane proteins: facing up to limited specificity. *Structure* **20,** 15–27 CrossRef Medline
21. DiNitto, J. P., and Lambright, D. G. (2006) Membrane and juxtamembrane targeting by PH and PTB domains. *Biochim. Biophys. Acta* **1761,** 850–867 CrossRef Medline
22. Roy, N. S., Yohe, M. E., Randazzo, P. A., and Gruschus, J. M. (2016) Allosteric properties of PH domains in Arf regulatory proteins. *Cell. Logist.* **6,** e1181700 CrossRef Medline
23. Musacchio, A., Gibson, T., Rice, P., Thompson, J., and Saraste, M. (1993) The PH domain–a common piece in the structural patchwork of signaling proteins. *Trends Biochem. Sci.* **18,** 343–348 CrossRef Medline
24. Scheffzek, K., and Welti, S. (2012) Pleckstrin homology (PH) like domains–versatile modules in protein–protein interaction platforms. *FEBS Lett.* **586,** 2662–2673 CrossRef Medline
25. Lemmon, M. A., and Ferguson, K. M. (2000) Signal-dependent membrane targeting by pleckstrin homology (PH) domains. *Biochem. J.* **350,** 1–18 CrossRef Medline
26. He, J., Scott, J. L., Heroux, A., Roy, S., Lenoir, M., Overduin, M., Stahelin, R. V., and Kutateladze, T. G. (2011) Molecular basis of phosphatidylinositol 4-phosphate and ARF1 GTPase recognition by the FAPP1 pleckstrin homology (PH) domain. *J. Biol. Chem.* **286,** 18650–18657 CrossRef Medline
27. Liu, Y., Kahn, R. A., and Prestegard, J. H. (2014) Interaction of Fapp1 with Arf1 and PI4P at a membrane surface: an example of coincidence detection. *Structure* **22,** 421–430 CrossRef Medline
28. Côte, M., Fos, C., Canonigo-Balancio, A. J., Ley, K., Bécart, S., and Altman, A. (2015) SLAT promotes TCR-mediated, Rap1-dependent LFA-1 activation and adhesion through interaction of its PH domain with Rap1. *J. Cell Sci.* **128,** 4341–4352 CrossRef Medline
29. Malaby, A. W., van den Berg, B., and Lambright, D. G. (2013) Structural basis for membrane recruitment and allosteric activation of cytohesin family Arf GTPase exchange factors. *Proc. Natl. Acad. Sci. U.S.A.* **110,** 14213–14218 CrossRef Medline
30. Cohen, L. A., Honda, A., Varnai, P., Brown, F. D., Balla, T., and Donaldson, J. G. (2007) Active Arf6 recruits ARNO/cytohesin GEFs to the PM by binding their PH domain. *Mol. Biol. Cell* **18,** 2244–2253 CrossRef Medline
31. Chen, Z., Gutowski, S., and Sternweis, P. C. (2018) Crystal structures of the PH domains from Lbc family of RhoGEFs bound to activated RhoA GTPase. *Data Brief* **17,** 356–362 CrossRef Medline
32. Bergamin, E., Hallock, P. T., Burden, S. J., and Hubbard, S. R. (2010) The cytoplasmic adaptor protein Dok7 activates the receptor tyrosine kinase MuSK via dimerization. *Mol. Cell* **39,** 100–109 CrossRef Medline
33. Vetter, I. R., Nowak, C., Nishimoto, T., Kuhlmann, J., and Wittinghofer, A. (1999) Structure of a Ran-binding domain complexed with Ran bound to a GTP analogue: implications for nuclear transport. *Nature* **398,** 39–46 CrossRef Medline
34. Snyder, J. T., Singer, A. U., Wing, M. R., Harden, T. K., and Sondek, J. (2003) The pleckstrin homology domain of phospholipase C-β2 as an effector site for Rac. *J. Biol. Chem.* **278,** 21099–21104 CrossRef Medline
35. Illenberger, D., Walliser, C., Nurnberg, B., Diaz Lorente, M., and Gierschik, P. (2003) Specificity and structural requirements of phospholipase C-β stimulation by Rho GTPases versus G protein $\beta\gamma$ dimers. *J. Biol. Chem.* **278,** 3006–3014 CrossRef Medline
36. Rojas, R. J., Yohe, M. E., Gershburg, S., Kawano, T., Kozasa, T., and Sondek, J. (2007) Gαq directly activates p63RhoGEF and Trio via a conserved extension of the Dbl homology-associated pleckstrin homology domain. *J. Biol. Chem.* **282,** 29201–29210 CrossRef Medline
37. Bellacosa, A., Chan, T. O., Ahmed, N. N., Datta, K., Malstrom, S., Stokoe, D., McCormick, F., Feng, J., and Tsichlis, P. (1998) Akt activation by growth factors is a multiple-step process: the role of the PH domain. *Oncogene* **17,** 313–325 CrossRef Medline
38. Chan, T. O., Rittenhouse, S. E., and Tsichlis, P. N. (1999) AKT/PKB and other D3 phosphoinositide-regulated kinases: kinase activation by phosphoinositide-dependent phosphorylation. *Annu. Rev. Biochem.* **68,** 965–1014 CrossRef Medline
39. DiNitto, J. P., Delprato, A., Gabe Lee, M. T., Cronin, T. C., Huang, S., Guilherme, A., Czech, M. P., and Lambright, D. G. (2007) Structural basis and mechanism of autoregulation in 3-phosphoinositide-dependent Grp1 family Arf GTPase exchange factors. *Mol. Cell* **28,** 569–583 CrossRef Medline
40. He, X., Kuo, Y. C., Rosche, T. J., and Zhang, X. (2013) Structural basis for autoinhibition of the guanine nucleotide exchange factor FARP2. *Structure* **21,** 355–364 CrossRef Medline
41. Soisson, S. M., Nimnual, A. S., Uy, M., Bar-Sagi, D., and Kuriyan, J. (1998) Crystal structure of the Dbl and pleckstrin homology domains from the human Son of sevenless protein. *Cell* **95,** 259–268 CrossRef Medline
42. Malaby, A. W., Das, S., Chakravarthy, S., Irving, T. C., Bilsel, O., and Lambright, D. G. (2018) Structural dynamics control allosteric activation of cytohesin family Arf GTPase exchange factors. *Structure* **26,** 106–117.e6 CrossRef Medline
43. Aizel, K., Biou, V., Navaza, J., Duarte, L. V., Campanacci, V., Cherfils, J., and Zeghouf, M. (2013) Integrated conformational and lipid-sensing regulation of endosomal ArfGEF BRAG2. *PLoS Biol.* **11,** e1001652 CrossRef Medline
44. Rossman, K. L., Worthylake, D. K., Snyder, J. T., Siderovski, D. P., Campbell, S. L., and Sondek, J. (2002) A crystallographic view of interactions between Dbs and Cdc42: PH domain-assisted guanine nucleotide exchange. *EMBO J.* **21,** 1315–1326 CrossRef Medline
45. Yoon, H. Y., Jacques, K., Nealon, B., Stauffer, S., Premont, R. T., and Randazzo, P. A. (2004) Differences between AGAP1, ASAP1 and arf GAP1 in substrate recognition: interaction with the N terminus of Arf1. *Cell. Signal.* **16,** 1033–1044 CrossRef Medline
46. Luo, R., Miller Jenkins, L. M., Randazzo, P. A., and Gruschus, J. (2008) Dynamic interaction between Arf GAP and PH domains of ASAP1 in the regulation of GAP activity. *Cell. Signal.* **20,** 1968–1977 CrossRef Medline
47. Northup, J. K., Jian, X., and Randazzo, P. A. (2012) Nucleotide exchange factors: kinetic analyses and the rationale for studying kinetics of GEFs. *Cell. Logist.* **2,** 140–146 CrossRef Medline
48. Randazzo, P. A., Jian, X., Chen, P.-W., Zhai, P., Soubias, O., and Northup, J. K. (2013) Quantitative analysis of guanine nucleotide exchange factors (GEFs) as enzymes. *Cell. Logist.* **3,** e27609 CrossRef Medline
49. Randazzo, P. A., and Kahn, R. A. (1995) Myristoylation and ADP-ribosylation factor function. *Methods Enzymol.* **250,** 394–405 CrossRef Medline
50. Randazzo, P. A., Terui, T., Sturch, S., Fales, H. M., Ferrige, A. G., and Kahn, R. A. (1995) The myristoylated amino terminus of ADP-ribosylation factor 1 is a phospholipid- and GTP-sensitive switch. *J. Biol. Chem.* **270,** 14809–14815 CrossRef Medline
51. Donaldson, J. G., and Jackson, C. L. (2011) ARF family G proteins and their regulators: roles in membrane transport, development and disease. *Nat. Rev. Mol. Cell Biol.* **12,** 362–375 CrossRef Medline
52. Randazzo, P. A. (1997) Functional interaction of ADP-ribosylation factor 1 with phosphatidylinositol 4,5-bisphosphate. *J. Biol. Chem.* **272,** 7688–7692 Medline
53. Terui, T., Kahn, R. A., and Randazzo, P. A. (1994) Effects of acid phospholipids on nucleotide exchange properties of ADP-ribosylation factor 1. Evidence for specific interaction with phosphatidylinositol 4,5-bisphosphate. *J. Biol. Chem.* **269,** 28130–28135 Medline
54. Luo, R., Jacques, K., Ahvazi, B., Stauffer, S., Premont, R. T., and Randazzo, P. A. (2005) Mutational analysis of the Arf1·GTP/Arf GAP interface reveals an Arf1 mutant that selectively affects the Arf GAP ASAP1. *Curr. Biol.* **15,** 2164–2169 CrossRef Medline
55. Campbell, R. B., Liu, F., and Ross, A. H. (2003) Allosteric activation of PTEN phosphatase by phosphatidylinositol 4,5-bisphosphate. *J. Biol. Chem.* **278,** 33617–33620 CrossRef Medline
56. Rebecchi, M. J., Eberhardt, R., Delaney, T., Ali, S., and Bittman, R. (1993) Hydrolysis of short acyl chain inositol lipids by phospholipase C-δ1. *J. Biol. Chem.* **268,** 1735–1741 Medline

57. Aguiar, J., Carpena, P., Molina-Bolivar, J. A., and Ruiz, C. C. (2003) On the determination of the critical micelle concentration by the pyrene 1:3 ratio method. *J. Colloid Interface Sci.* **258,** 116–122 CrossRef
58. Seidel, R. D., 3rd., Amor, J. C., Kahn, R. A., and Prestegard, J. H. (2004) Structural perturbations in human ADP ribosylation factor-1 accompanying the binding of phosphatidylinositides. *Biochemistry* **43,** 15393–15403 CrossRef Medline
59. Lakowicz, J. R. (2006) *Principles of Fluorescence Spectroscopy*, 3rd Ed., pp. 361–363, Springer, New York
60. Yasgar, A., Jadhav, A., Simeonov, A., and Coussens, N. P. (2016) AlphaScreen-based assays: ultra-high-throughput screening for small-molecule inhibitors of challenging enzymes and protein-protein interactions. *Methods Mol. Biol.* **1439,** 77–98 CrossRef Medline
61. Li, Y., Soubias, O., Li, J., Sun, S., Randazzo, P. A., and Byrd, R. A. (2019) Functional expression and characterization of human myristoylated-Arf1 in nanodisc membrane mimetics. *Biochemistry* **58,** 1423–1431 CrossRef Medline
62. Rossman, K. L., Cheng, L., Mahon, G. M., Rojas, R. J., Snyder, J. T., Whitehead, I. P., and Sondek, J. (2003) Multifunctional roles for the PH domain of Dbs in regulating Rho GTPase activation. *J. Biol. Chem.* **278,** 18393–18400 CrossRef Medline
63. Blomberg, N., Baraldi, E., Nilges, M., and Saraste, M. (1999) The PH superfold: a structural scaffold for multiple functions. *Trends Biochem. Sci.* **24,** 441–445 CrossRef Medline
64. Yun, M., Keshvara, L., Park, C. G., Zhang, Y. M., Dickerson, J. B., Zheng, J., Rock, C. O., Curran, T., and Park, H. W. (2003) Crystal structures of the DAB homology domains of mouse disabled 1 and 2. *J. Biol. Chem.* **278,** 36572–36581 CrossRef Medline
65. Stolt, P. C., Vardar, D., and Blacklow, S. C. (2004) The dual-function disabled-1 PTB domain exhibits site independence in binding phosphoinositide and peptide ligands. *Biochemistry* **43,** 10979–10987 CrossRef Medline
66. Vetter, I. R., and Wittinghofer, A. (2001) Signal transduction–the guanine nucleotide-binding switch in three dimensions. *Science* **294,** 1299–1304 CrossRef Medline
67. Sprang, S. R. (1997) G protein mechanisms: insights from structural analysis. *Annu. Rev. Biochem.* **66,** 639–678 CrossRef Medline
68. Kahn, R. A., Cherfils, J., Elias, M., Lovering, R. C., Munro, S., and Schurmann, A. (2006) Nomenclature for the human Arf family of GTP-binding proteins: ARF, ARL, and SAR proteins. *J. Cell Biol.* **172,** 645–650 CrossRef Medline
69. Kahn, R. A., Randazzo, P., Serafini, T., Weiss, O., Rulka, C., Clark, J., Amherdt, M., Roller, P., Orci, L., and Rothman, J. E. (1992) The amino terminus of ADP-ribosylation factor (ARF) is a critical determinant of ARF activities and is a potent and specific inhibitor of protein transport. *J. Biol. Chem.* **267,** 13039–13046 Medline
70. Randazzo, P. A., Terui, T., Sturch, S., and Kahn, R. A. (1994) The amino terminus of ADP-ribosylation factor (ARF) 1 is essential for interaction with Gs and ARF GTPase-activating protein. *J. Biol. Chem.* **269,** 29490–29494 Medline
71. Balch, W. E., Kahn, R. A., and Schwaninger, R. (1992) ADP-ribosylation factor is required for vesicular trafficking between the endoplasmic reticulum and the cis-Golgi compartment. *J. Biol. Chem.* **267,** 13053–13061 Medline
72. Liu, Y., Kahn, R. A., and Prestegard, J. H. (2009) Structure and membrane interaction of myristoylated ARF1. *Structure* **17,** 79–87 CrossRef Medline
73. Jian, X., Gruschus, J. M., Sztul, E., and Randazzo, P. A. (2012) The pleckstrin homology (PH) domain of the Arf exchange factor Brag2 is an allosteric binding site. *J. Biol. Chem.* **287,** 24273–24283 CrossRef Medline
74. Zhang, T., Li, S., Zhang, Y., Zhong, C., Lai, Z., and Ding, J. (2009) Crystal structure of the ARL2–GTP–BART complex reveals a novel recognition and binding mode of small GTPase with effector. *Structure* **17,** 602–610 CrossRef Medline
75. Gorfe, A. A., Hanzal-Bayer, M., Abankwa, D., Hancock, J. F., and McCammon, J. A. (2007) Structure and dynamics of the full-length lipid-modified H-ras protein in a 1,2-dimyristoylglycero-3-phosphocholine bilayer. *J. Med. Chem.* **50,** 674–684 CrossRef Medline
76. Abankwa, D., Gorfe, A. A., and Hancock, J. F. (2008) Mechanisms of Ras membrane organization and signaling: Ras on a rocker. *Cell Cycle* **7,** 2667–2673 CrossRef Medline
77. Abankwa, D., Hanzal-Bayer, M., Ariotti, N., Plowman, S. J., Gorfe, A. A., Parton, R. G., McCammon, J. A., and Hancock, J. F. (2008) A novel switch region regulates H-ras membrane orientation and signal output. *EMBO J.* **27,** 727–735 CrossRef Medline
78. Ismail, S. A., Chen, Y. X., Rusinova, A., Chandra, A., Bierbaum, M., Gremer, L., Triola, G., Waldmann, H., Bastiaens, P. I., and Wittinghofer, A. (2011) Arl2-GTP and Arl3-GTP regulate a GDI-like transport system for farnesylated cargo. *Nat. Chem. Biol.* **7,** 942–949 CrossRef Medline
79. Dharmaiah, S., Bindu, L., Tran, T. H., Gillette, W. K., Frank, P. H., Ghirlando, R., Nissley, D. V., Esposito, D., McCormick, F., Stephen, A. G., and Simanshu, D. K. (2016) Structural basis of recognition of farnesylated and methylated KRAS4b by PDEδ. *Proc. Natl. Acad. Sci. U.S.A.* **113,** E6766–E6775 CrossRef Medline
80. Che, M. M., Nie, Z., and Randazzo, P. A. (2005) Assays and properties of the Arf GAPs AGAP1, ASAP1, and Arf GAP1. *Methods Enzymol.* **404,** 147–163 CrossRef Medline
81. Ha, V. L., Thomas, G. M., Stauffer, S., and Randazzo, P. A. (2005) Preparation of myristoylated Arf1 and Arf6. *Methods Enzymol.* **404,** 164–174 CrossRef Medline
82. Chen, P. W., Jian, X., Luo, R., and Randazzo, P. A. (2012) Approaches to studying Arf GAPs in cells: *in vitro* assay with isolated focal adhesions. *Curr. Protoc. Cell Biol.* 2012, Chapter 17, Unit 17.13 CrossRef Medline
83. Luo, R., Ha, V. L., Hayashi, R., and Randazzo, P. A. (2009) Arf GAP2 is positively regulated by coatomer and cargo. *Cell. Signal.* **21,** 1169–1179 CrossRef Medline
84. Luo, R., and Randazzo, P. A. (2008) Kinetic analysis of Arf GAP1 indicates a regulatory role for coatomer. *J. Biol. Chem.* **283,** 21965–21977 CrossRef Medline
85. Bigay, J., Gounon, P., Robineau, S., and Antonny, B. (2003) Lipid packing sensed by ArfGAP1 couples COPI coat disassembly to membrane bilayer curvature. *Nature* **426,** 563–566 CrossRef Medline
86. Hall, M. D., Yasgar, A., Peryea, T., Braisted, J. C., Jadhav, A., Simeonov, A., and Coussens, N. P. (2016) Fluorescence polarization assays in high-throughput screening and drug discovery: a review. *Methods Appl. Fluoresc.* **4,** 022001 CrossRef Medline
87. Brodie, N. I., Popov, K. I., Petrotchenko, E. V., Dokholyan, N. V., and Borchers, C. H. (2017) Solving protein structures using short-distance cross-linking constraints as a guide for discrete molecular dynamics simulations. *Sci. Adv.* **3,** e1700479 CrossRef Medline
88. Yang, B., Wu, Y. J., Zhu, M., Fan, S. B., Lin, J., Zhang, K., Li, S., Chi, H., Li, Y. X., Chen, H. F., Luo, S. K., Ding, Y. H., Wang, L. H., Hao, Z., Xiu, L. Y., *et al.* (2012) Identification of cross-linked peptides from complex samples. *Nat. Methods* **9,** 904–906 CrossRef Medline
89. Hagn, F., Etzkorn, M., Raschle, T., and Wagner, G. (2013) Optimized phospholipid bilayer nanodiscs facilitate high-resolution structure determination of membrane proteins. *J. Am. Chem. Soc.* **135,** 1919–1925 CrossRef Medline
90. Pettersen, E. F., Goddard, T. D., Huang, C. C., Couch, G. S., Greenblatt, D. M., Meng, E. C., and Ferrin, T. E. (2004) UCSF Chimera–a visualization system for exploratory research and analysis. *J. Comput. Chem.* **25,** 1605–1612 CrossRef Medline